

# Structure of odd–odd Ga and As nuclei, and dynamical and supersymmetries

T. Fényes, A. Algora, Zs. Podolyák, D. Sohler, and J. Timár

*Institute of Nuclear Research of the Hungarian Academy of Science, 4001 Debrecen, Hungary*

S. Brant, V. Paar, and Lj. Šimičić

*Department of Physics, Faculty of Science, University of Zagreb, 41000 Zagreb, Croatia*

Fiz. Élem. Chastits At. Yadra **26**, 831–872 (July–August 1995)

The structure of  $^{66}\text{Ga}$ ,  $^{68}\text{Ga}$ ,  $^{70}\text{Ga}$ ,  $^{70}\text{As}$ ,  $^{72}\text{As}$ ,  $^{73}\text{As}$ ,  $^{74}\text{As}$ , and  $^{76}\text{As}$  is studied via  $(p, n\gamma)$  [and in some cases  $(\alpha, n\gamma)$ ] reactions. In-beam  $\gamma$ -ray, two-dimensional  $\gamma\gamma$ -coincidence, internal-conversion electron, and  $\gamma$ -ray angular-distribution spectra, as well as  $\sigma(E_{\text{LEV}}, E_p)$  relative reaction cross sections are measured with Ge(HP), Ge(Li)  $\gamma$  and combined superconducting-magnetic plus Si(Li) electron spectrometers at different bombarding-particle energies. The proposed new level schemes contain 300 (among them 70 new) levels. Level spins, parities, and  $\gamma$ -ray branching and mixing ratios are deduced. Energy spectra, electromagnetic moments, reduced transition probabilities,  $\gamma$ -ray branching ratios, and one-nucleon transfer reaction spectroscopic factors are calculated in the framework of the interacting boson model (IBM), the interacting boson–fermion model (IBFM), and the interacting boson–fermion–fermion model (IBFFM) for about 20 nuclei in the Ga–As region ( $^{64-67}\text{Zn}$ ,  $^{65-68}\text{Ga}$ ,  $^{68-73}\text{Ge}$ ,  $^{70-74}\text{As}$ ). The odd–odd nuclei are described on the basis of a consistent parametrization deduced from the even–even core and the two neighboring odd- $A$  nuclei. A reasonable description of the experimental data is obtained. The energy splitting of proton–neutron multiplets in odd–odd Ga and As nuclei is discussed by the use of the parabolic rule associated with the IBFFM in low perturbation order. The energy spectra of  $^{74}\text{Se}_{40}$ ,  $^{75}\text{Se}_{41}$ ,  $^{73}\text{As}_{40}$ ,  $^{74}\text{As}_{41}$  supermultiplet nuclei are calculated on the basis of the  $U_\pi(6/12) \otimes U_\nu(6/12)$  supersymmetry (SUSY) theory, using a simple closed energy formula; 44 states of these four different nuclei are reasonably described with only seven fitted parameters. The existence of supersymmetry is supported also by one–nucleon transfer reaction data, electromagnetic properties, and IBFM, IBFFM and SUSY model wave functions of the levels considered. © 1995 American Institute of Physics.

## 1. INTRODUCTION

The main intention of the present work was to make a detailed in-beam  $\gamma$ - and electron-spectroscopic study of the odd–odd Ga and As isotopes and to give a consistent description of the structure of the Zn, Ga, Ge, and As nuclei in the framework of the interacting boson (boson–fermion–fermion) model [IB(FF)M]. The nuclei investigated in this program are shown in Fig. 1.

The experimental work was motivated by the fact that the level systems of the investigated odd–odd nuclei (and especially the level spin and parity values) were known very scantily. For example, in  $^{68}\text{Ga}$  unambiguous spin–parity data had been determined only for three levels before our measurements. The beams of the Debrecen isochronous cyclotron enabled excitation of both particle and collective states, and the high-resolution, high-efficiency Ge(HP) detectors and unique superconducting magnetic electron spectrometer, constructed at the Institute of Nuclear Research, assured a

good possibility for complex  $\gamma$ - and electron-spectroscopic in-beam studies.

A theoretical interpretation of the  $^{66}\text{Ga}$  and  $^{68}\text{Ga}$  level schemes was formerly completely missing. In the case of  $^{70,72,74}\text{As}$  we have performed calculations in the interacting boson–fermion–fermion model for the first time. These calculations give a consistent and detailed description of the energy spectra and electromagnetic properties of the corresponding even–even, odd- $A$  and odd–odd Zn, Ga, Ge, and As nuclei.

The new experimental data obtained on  $^{73}\text{As}$  and  $^{74}\text{As}$  offered a possibility of checking the supersymmetry predictions for  $^{74}\text{Se}$ ,  $^{75}\text{Se}$ ,  $^{73}\text{As}$ , and  $^{74}\text{As}$  nuclei.

## 2. EXPERIMENTAL METHODS AND RESULTS

We have studied the excited states of the Ga and As nuclei in the proton and  $\alpha$ -particle beams of the Debrecen

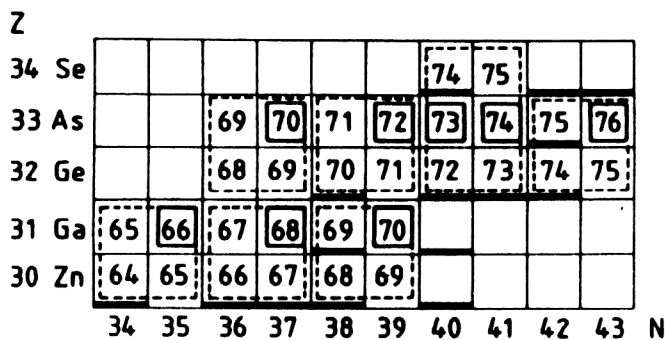


FIG. 1. Nuclei investigated in this program experimentally are indicated by eight mass numbers in solid frames. Mass numbers in dotted frames: theoretical calculations.  $Z$ : atomic;  $N$ : neutron numbers; mass number underlined with a thick line: stable nucleus.

103-cm (and in some experiments of the Jyväskylä 90-cm) isochronous cyclotrons via  $(p, n\gamma)$  and  $(\alpha, n\gamma)$  reactions. The targets were prepared from enriched Cu, Zn, and Ge isotopes. The description of the spectroscopic channels of the Debrecen cyclotron can be found in Refs. 1 and 2.

High-resolution Ge (HP and LEPS) detectors were used for a  $\gamma$  and superconducting magnetic lens plus Si(Li) spectrometer (SMLS) for electron-spectroscopic measurements. The SML spectrometer, which was described in detail in Ref. 3, has high transmission, good energy resolution, and low background.

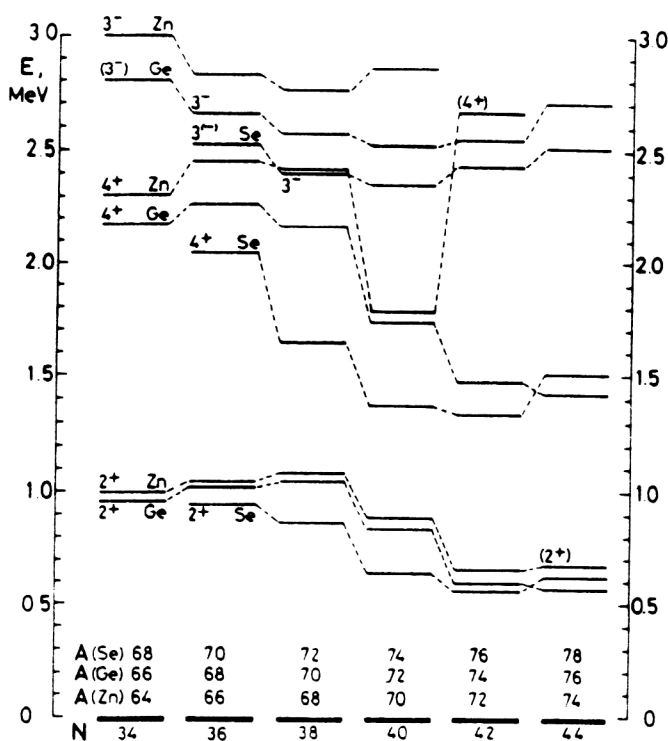
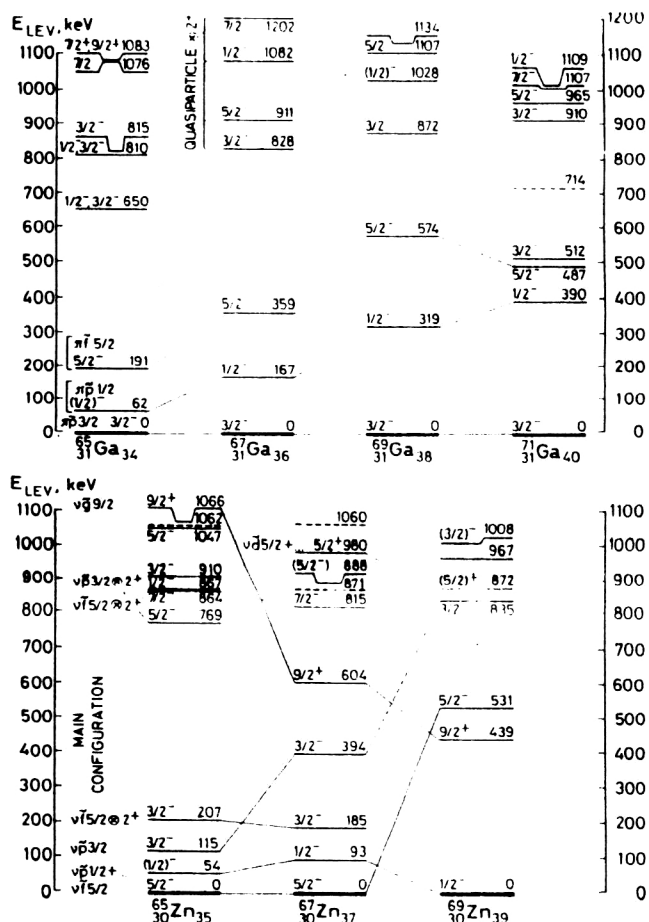


FIG. 2. Energies of  $2_1^+$ ,  $4_1^+$ , and  $3_1^-$  states of the even-even Zn, Ge, and Se nuclei. Data were taken from the corresponding Nuclear Data Sheets.

In order to obtain "complete" spectroscopic information,  $\gamma$ -ray ( $E_\gamma, I_\gamma$ ),  $\gamma\gamma$ -coincidence, internal-conversion electron, and  $\gamma$ -ray angular-distribution spectra, as well as the relative reaction cross section  $\sigma_{\text{rel}}(E_{\text{LEV}}, E_p)$  were measured at different bombarding-particle energies. Level schemes, spin-parity values, and  $\gamma$ -branching and  $\gamma$ -mixing ratios have been deduced. Great attention was paid to the reliability and consistency of the experimental data. For example, the level spins have been determined with three different methods: a) from the decay properties and internal-conversion coefficients of transitions; b) from a Hauser-Feshbach analysis of the  $(p, n)$  reaction cross sections; c) from  $\gamma$ -ray angular distributions. The configuration of levels has been determined from all available data: from nucleon-transfer reaction studies,  $\log ft$  values of  $\beta$  decay, electromagnetic moments, transition probabilities,  $\gamma$ -branching ratios, predictions of parabolic-rule calculations, etc.

As a result of experimental work about 880 (among them 440 new)  $\gamma$  rays have been identified, and 280 (including 240 new)  $\alpha_K$  internal-conversion coefficients and  $\sim 300$  (among them 70 new) levels have been determined in  $^{66,68,70}\text{Ga}$  and  $^{70,72,73,74,76}\text{As}$  nuclei.

The results have been published in the following papers:  $^{66}\text{Ga}$  (Refs. 4 and 13),  $^{68}\text{Ga}$  (Refs. 5, 6, and 13),  $^{70}\text{Ga}$  (Ref.





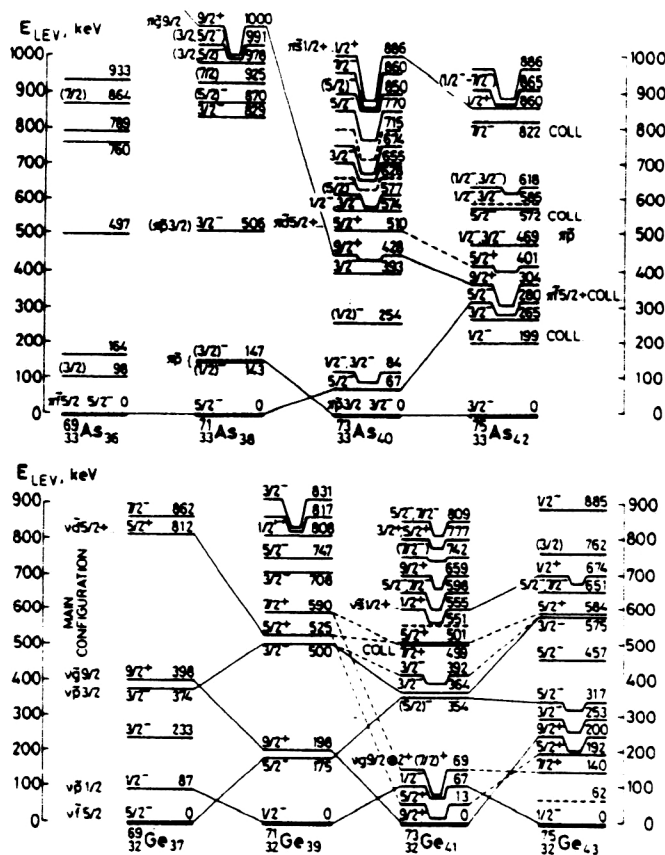


FIG. 4. The low-lying levels of odd- $A$   $^{69-75}\text{Ge}$  and  $^{69-75}\text{As}$  nuclei. Data were taken from the corresponding Nuclear Data Sheets and original papers.

7),  $^{70}\text{As}$  (Ref. 8),  $^{72}\text{As}$  (Refs. 9 and 13),  $^{73}\text{As}$  (Ref. 10),  $^{74}\text{As}$  (Refs. 11–13), and  $^{76}\text{As}$  (Ref. 14). These papers contain detailed descriptions of the experimental methods and results, deduced new level schemes, and their discussion. The level spectra were based mainly on  $\gamma\gamma$ -coincidence relations, as well as on the energy and intensity balance of the transitions.

### 3. SYSTEMATICS OF THE EVEN-EVEN AND SINGLE-ODD NUCLEI IN THE Zn–Se REGION

If we want to describe the structure of odd–odd nuclei, we need to know the energy levels of the neighboring even–even and odd- $A$  nuclei. The systematics of the  $0_1^+$ ,  $2_1^+$ ,  $4_1^+$ , and  $3_1^-$  states of the even–even Zn, Ge, and Se nuclei is shown in Fig. 2. The low-lying levels of the odd- $A$  Zn, Ga and Ge, As nuclei are presented in Figs. 3 and 4, respectively. The main configurations of states are also indicated in Figs. 3 and 4 on the basis of the one-nucleon transfer reaction and other available data.

The systematics of neutron quasiparticle energies and occupation probabilities in the Ni–Se region are shown in Fig. 5.

In order to get preliminary estimates for the configurations of the low-lying levels of odd–odd Ga and As nuclei, we have performed parabolic-rule<sup>16</sup> calculations. These calculations proved very useful for the prediction of the energy splitting of different proton–neutron multiplets in odd–odd

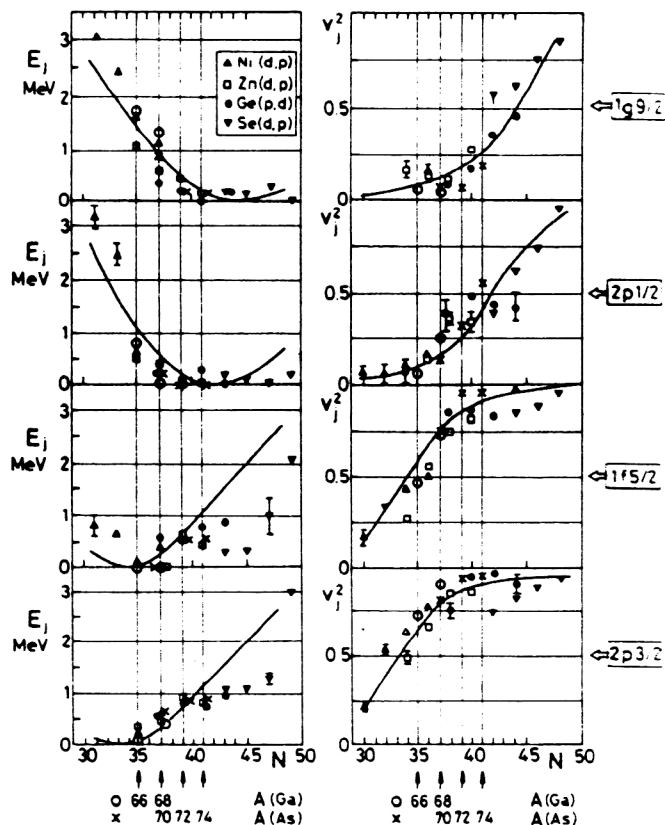


FIG. 5. Experimental quasiparticle energies ( $E_j$ ) and occupation probabilities ( $v_j$ ) as a function of the neutron number ( $N$ ) (points) and the corresponding BCS theoretical results (curves). Data were taken from Fournier *et al.*<sup>15</sup> Values used in the present calculations are shown by circles (O) for Ga and crosses (x) for As odd–odd nuclei.

In (Ref. 1) and Sb (Ref. 2) nuclei. In the Ga and As isotopes rather strong configuration mixing is expected among the close-lying identical spin–parity states, which may imply a limitation on the applicability of the parabolic rule. Nevertheless, it can be used for the first orientation, as indeed the IBFFM calculations showed later.

As the parabolic rule and its applications to In and Sb nuclei were described in detail in Refs. 1, 2, and 16, here we show only the results obtained on the relative energy splitting of proton–neutron multiplets in  $^{70}\text{As}$  (Fig. 6) and  $^{66,68,70}\text{Ga}$ ,  $^{70,72,74,76}\text{As}$  nuclei (Fig. 7). For these predictions the same proton and neutron occupation probabilities were used, as later in the IBFFM calculations (see Sec. 4).

### 4. INTERACTING BOSON AND BOSON–FERMION–FERMION MODEL CALCULATIONS

In order to get deeper and more detailed insight into the structure of the low-lying odd–odd Ga and As states, we have calculated the level energies and electromagnetic properties on the basis of the interacting boson (boson–fermion–fermion) model.

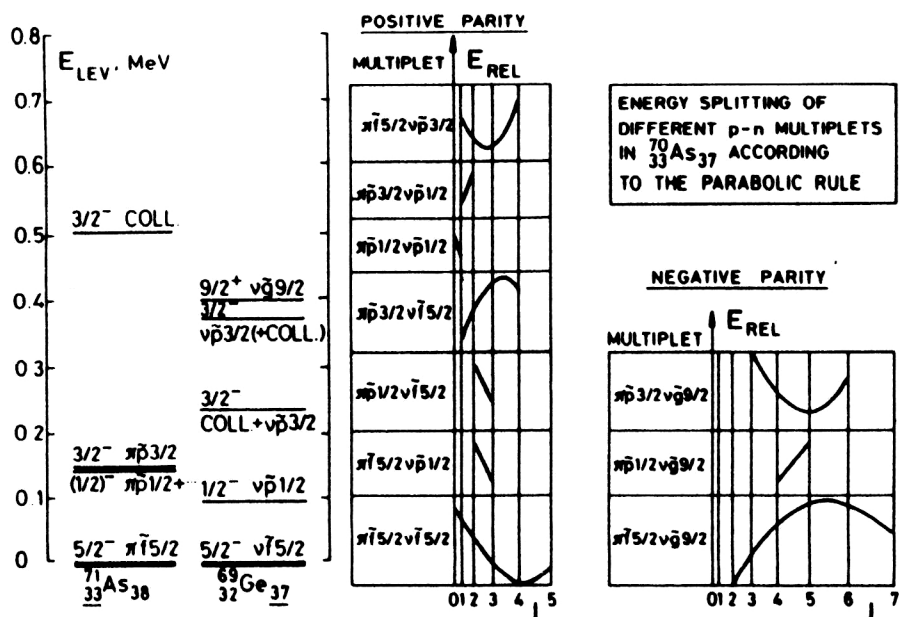


FIG. 6. Approximate relative energy splitting of different proton-neutron multiplets in  $^{70}\text{As}_{37}$ , as predicted by the parabolic rule. The abscissa is scaled according to  $J(J+1)$ , where  $J$  is the spin of the state.

#### 4.1. Hamilton operator

The Hamiltonian of the model is<sup>17-20</sup>

$$H_{\text{IBFM}} = H_{\text{IBFM}}(\pi) + H_{\text{IBFM}}(\nu) - H_{\text{IBM}} + H_{\text{RES}}(\pi\nu), \quad (1)$$

where  $H_{\text{IBM}}$  denotes the IBM Hamiltonian for the even-even core nucleus,<sup>21,22</sup>  $H_{\text{IBFM}}(\pi)$  and  $H_{\text{IBFM}}(\nu)$  are the IBFM Hamiltonians for the neighboring odd-even nuclei with an odd proton and odd neutron, respectively,<sup>23-25</sup> and  $H_{\text{RES}}(\pi\nu)$  is the Hamiltonian of the residual interaction.

The Hamiltonian of the core has the form<sup>26-28</sup>

$$H_{\text{IBM}} = h_1 \hat{N} + h_2 \{ (d^+ d^+)_{0,0} [(N - \hat{N})(N - \hat{N} - 1)]^{1/2} + \text{H.c.} \} + h_3 \{ (d^+ d^+ \tilde{d})_{0,0} (N - \hat{N})^{1/2} + \text{H.c.} \}$$

$$+ \sum_{L=0,2,4} h_{4L} [(d^+ d^+)_{L,0} (\tilde{d} \tilde{d})_{L,0}]_0, \quad (2)$$

where  $\hat{N}$  is the  $d$ -boson number operator and  $N$  is the total number of  $s$  and  $d$  bosons. The relation of the  $\{h\}$  parameters to the parameters defined in Ref. 21 is as follows:

MULTIPLY	PA-RITY	$^{66}\text{Ga}_{35}$	$^{68}\text{Ga}_{37}$	$^{70}\text{Ga}_{39}$	$^{70}\text{As}_{37}$	$^{72}\text{As}_{39}$	$^{74}\text{As}_{41}$	$^{76}\text{As}_{43}$
$\pi 3/2 \nu 9/2$	-	U	U	U	U	U	U	U
$\pi 3/2 \nu 1/2$	+	/	/	/	/	/	/	/
$\pi 3/2 \nu 5/2$	+	U	U	U	U	U	U	U
$\pi 3/2 \nu 3/2$	+	U	U	U	U	U	U	U
$\pi 15/2 \nu 9/2$	-	U	U	U	U	U	U	U
$\pi 15/2 \nu 1/2$	+	/	/	/	/	/	/	/
$\pi 15/2 \nu 5/2$	+	U	U	U	U	U	U	U
$\pi 15/2 \nu 3/2$	+	U	U	U	U	U	U	U
$\pi 1/2 \nu 9/2$	-	/	/	/	/	/	/	/
$\pi 1/2 \nu 1/2$	+	/	/	/	/	/	/	/
$\pi 1/2 \nu 5/2$	+	/	/	/	/	/	/	/
$\pi 1/2 \nu 3/2$	+	/	/	/	/	/	/	/
$\pi 9/2 \nu 9/2$	+	U	U	U	U	U	U	U
$\pi 9/2 \nu 1/2$	-	/	/	/	/	/	/	/
$\pi 9/2 \nu 5/2$	-	U	U	U	U	U	U	U
$\pi 9/2 \nu 3/2$	-	U	U	U	U	U	U	U

FIG. 7. Approximate relative energy splitting of different proton-neutron multiplets in some odd-odd Ga and As nuclei as a function of  $J(J+1)$ , where  $J$  is the spin of the state. The predictions are based on the parabolic rule.

TABLE I. Parameters of the IBFFM calculations.

Parameters		$^{60}_{31}\text{Ga}_{15}$	$^{68}_{31}\text{Ga}_{17}$	$^{70}_{33}\text{As}_{17}$	$^{72}_{33}\text{As}_{19}$	$^{74}_{33}\text{As}_{21}$
Core, MeV	$h_1$	0.8	1.039	0.9	0.88	0.68
	$h_2$	-0.2	0	-0.15	-0.3	-0.25
	$h_3$	0	0	0.06	0.12	0.1
	$h_{40}$	0.1	0.147	0	0.2	0
	$h_{42}$	-0.15	-0.2292	-0.5	-0.4	-0.3
	$h_{44}$	0.3	0.5595	-0.08	-0.08	-0.08
Total boson $N^0$ ,	$N$	4	5	3	4 (or 7)	4
	$\chi$	-0.5	-0.5	-1.323*	-1.323*	-1.323*
$e$	$e^{\text{vib}}$	1.35	1.35	0.8	0.8	0.8
Quasi-proton energy, MeV	$E(\pi p 3/2)$	0	0	0.3	0	0
	$E(\pi f 5/2)$	0.75	0.75	0	0.41	0.41
	$E(\pi p 1/2)$	0.615	0.615	0.3	0.74	0.74
	$E(\pi g 9/2)$			1.3	2.2	1.55
	$E(\pi d 5/2)$				5.2	4.55
Occup. probability	$V^2(\pi p 3/2)$	0.6	0.6	0.607	0.607	0.579
	$V^2(\pi f 5/2)$	0.07	0.07	0.309	0.309	0.341
	$V^2(\pi p 1/2)$	0.09	0.09	0.131	0.131	0.118
	$V^2(\pi g 9/2)$			0.07	0.07	0.06
	$V^2(\pi d 5/2)$				0.01	0.01
Quasi-neutron energy, MeV	$E(\nu p 3/2)$	0.09	0.49	0.60	0.95	0.95
	$E(\nu f 5/2)$	0	0	0	0.53	0.53
	$E(\nu p 1/2)$	0.83	0.03	0.2	0	0
	$E(\nu g 9/2)$	1.69	1.36	0.9	0.2	0.2
	$E(\nu d 5/2)$				3.2	3.2
Occup. probability	$V^2(\nu p 3/2)$	0.73	0.89	0.80	0.941	0.957
	$V^2(\nu f 5/2)$	0.48	0.73	0.75	0.949	0.962
	$V^2(\nu p 1/2)$	0.11	0.25	0.16	0.327	0.624
	$V^2(\nu g 9/2)$	0.08	0.04	0.09	0.09	0.217
	$V^2(\nu d 5/2)$				0.01	0.01
Strengths of boson-fermion interaction, MeV	$\Lambda_0^{\pi}$	0.05	0.05	0.05	0.05	0.05
	$\Gamma_0^{\pi}$	0.48	0.4	0.4	0.5	0.5
	$\Lambda_0^{\pi}$	1.4	0.5	0.5	$0.5\pi +$	0.5
	$\Lambda_0^{\nu}$	0	0	0	$1.5\pi -$	0
	$\Gamma_0^{\nu}$	0.02	0.15	0.2	$0.55\pi +$	0.55
	$\Lambda_0^{\nu}$	1.63	1.3	1.3	$0.45\pi -$	
					$1.30\pi +$	$1.3\pi +$
					$5.50\pi -$	$5.5\pi -$
Effective gyromagn. ratios	$g_i^{\pi}$	$0.4g_i^{\pi}/\square$	$0.4g_i^{\pi}/\square$	$0.40g_i^{\pi}/\pi +$ $0.65g_i^{\pi}/\pi -$	$0.7g_i^{\pi}/\square$	$0.7g_i^{\pi}/\square$
	$g_{\text{tens}}^{\pi **}$	1.56	1.59 <sup>o</sup>	0	3.340	3.372
	$g_i^{\nu}$	$0.9g_i^{\nu}/\nabla$	$0.5g_i^{\nu}/\pi +$ $0.9g_i^{\nu}/\pi -$	$0.4g_i^{\nu}/\square$	$0.7g_i^{\nu}/\square$	$0.7g_i^{\nu}/\square$
Strengths of residual interaction, MeV	$V_{\delta}$	-0.4	-0.4	$0\pi +$	$0\pi +$	$0\pi +$
	$V_{\sigma\sigma}$	0.4	0.4	$-0.4\pi -$ $0.4\pi +$	$-0.6\pi -$ 0	$-0.6\pi -$ 0
	$V_{\text{tens}}$	-0.01	0.015	$0.3\pi -$ 0.015	0.015	0.015

$e^{\pi}=1.5e$ ,  $e^{\nu}=0.5e$ ,  $g_l^{\pi}=1$ ,  $g_l^{\nu}=0$ ,  $g_R=Z/A$  in all cases.

\*1.323= $\sqrt{7/2}$ .

$\pi+$  and  $\pi-$  stand for positive- and negative-parity states, respectively.

\*\*The tensor gyromagnetic ratio,  $g_{\text{tens}}^{\pi,\nu}$  (Refs. 59 and 60) is similar to the one used in Ref. 61.

$\square \frac{1}{50}\langle r^2 \rangle g_s^{\pi}(\text{free})=1.59$ ;  $\triangle \frac{1}{50}\langle r^2 \rangle g_s^{\nu}(\text{free})=-1.09$ .

$\square g_s^{\pi,f}=g_s^{\pi}(\text{free})=5.5857$ .

$\nabla g_s^{\nu,f}=g_s^{\nu}(\text{free})=-3.8263$ .

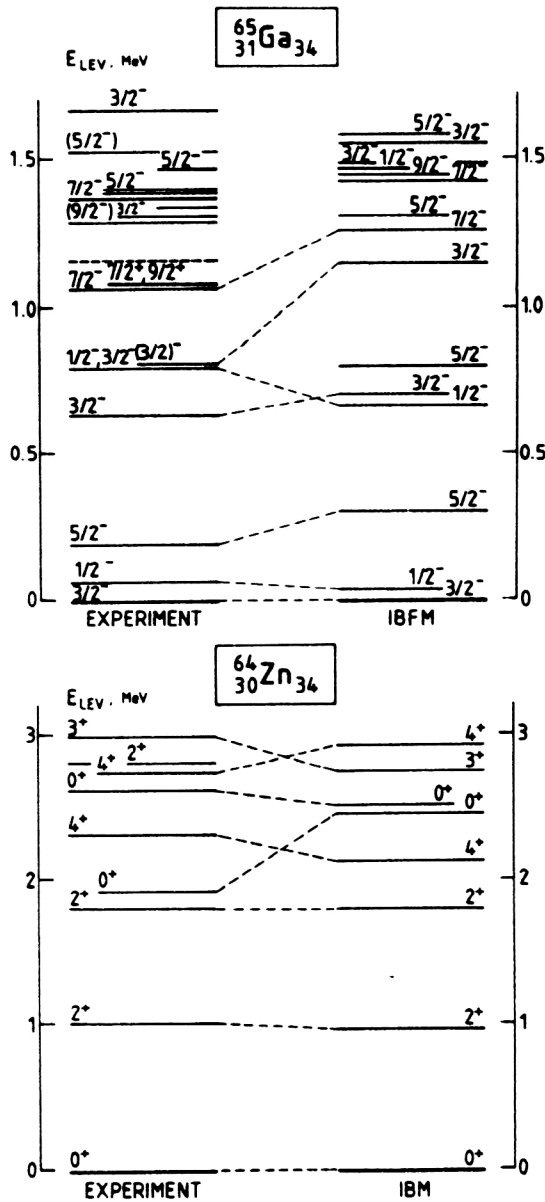


FIG. 8. Experimental energy spectra of  $^{64}\text{Zn}$  (Ref. 30) and  $^{65}\text{Ga}$  (Ref. 31) and the corresponding theoretical IBM and IBFM results.<sup>4</sup>

$$\begin{aligned}
 h_1 &= \epsilon_d - \epsilon_s + \left( \frac{1}{\sqrt{5}} u_2 - u_0 \right) (N-1), \\
 h_2 &= \frac{1}{\sqrt{2}} \tilde{v}_0, \quad h_3 = \tilde{v}_2, \\
 h_{4L} &= \sqrt{2L+1} \left( \frac{1}{2} c_L - \frac{1}{\sqrt{5}} u_2 + \frac{1}{2} u_0 \right).
 \end{aligned} \quad (3)$$

The IBFM Hamiltonian employed here is of the form<sup>27</sup>

$$H_{\text{IBFM}}(\alpha) = H_{\text{IBM}} + \sum_i \tilde{\epsilon}_i(\alpha) + H_{\text{BF}}(\alpha), \quad (4)$$

where  $\alpha$  stands for an odd proton ( $\alpha = \pi$ ) or neutron ( $\alpha = \nu$ ). The second and third terms are the quasiparticle and boson–fermion (particle–vibration) interaction Hamiltonians, respectively, and

$$\begin{aligned}
 H_{\text{BF}}(\alpha) &= \sum_j A_j \{ (d^+ \tilde{d})_0 [c_j^+(\alpha) \tilde{c}_j(\alpha)]_0 \}_0 \\
 &+ \sum_{j_1 j_2} \Gamma_{j_1 j_2} \{ Q_2 [c_{j_1}^+(\alpha) \tilde{c}_{j_2}(\alpha)]_2 \}_0 \\
 &+ \sum_{j_1 j_2 j_3} \Lambda_{j_1 j_2 j_3} \{ [c_{j_1}^+(\alpha) \tilde{d}]_{j_3} [\tilde{c}_{j_2}(\alpha) d^+]_{j_3} \}_0, \quad (5)
 \end{aligned}$$

with

$$A_j = A_0 \sqrt{5(2j+1)}, \quad (6)$$

$$\Gamma_{j_1 j_2} = \Gamma_0 \sqrt{5} (u_{j_1} u_{j_2} - v_{j_1} v_{j_2}) \langle j_1 \| Y_2 \| j_2 \rangle, \quad (7)$$

$$\begin{aligned}
 \Lambda_{j_1 j_2 j_3} &= -2\Lambda_0 \frac{\sqrt{5}}{\sqrt{2j_3+1}} (u_{j_1} v_{j_3} + v_{j_1} u_{j_3}) \\
 &\times (u_{j_3} v_{j_2} + v_{j_3} u_{j_2}) \cdot \langle j_3 \| Y_2 \| j_1 \rangle \langle j_3 \| Y_2 \| j_2 \rangle, \quad (8)
 \end{aligned}$$

$$Q_{2\mu} = d_\mu^+ \sqrt{N - \tilde{N}} + \sqrt{N - \tilde{N}} \tilde{d}_\mu + \chi (d^+ \tilde{d})_{2\mu}. \quad (9)$$

The Hamiltonian of the residual interaction was taken in the form

$$\begin{aligned}
 H_{\text{RES}}(\pi\nu) &= 4\pi V_\delta \delta(\mathbf{r}_\pi - \mathbf{r}_\nu) \delta(r_\pi - R_0) - \sqrt{3} V_{\sigma\sigma} (\boldsymbol{\sigma}_\pi \cdot \boldsymbol{\sigma}_\nu) \\
 &+ V_{\text{tens}} \left[ \frac{3(\boldsymbol{\sigma}_\pi \cdot \mathbf{r}_{\pi\nu})(\boldsymbol{\sigma}_\nu \cdot \mathbf{r}_{\pi\nu})}{r_{\pi\nu}^2} - (\boldsymbol{\sigma}_\pi \cdot \boldsymbol{\sigma}_\nu) \right], \quad (10)
 \end{aligned}$$

where  $\mathbf{r}_{\pi\nu} = \mathbf{r}_\pi - \mathbf{r}_\nu$ ,  $R_0 = 1.2\sqrt[3]{A}$  fm;  $H_{\text{RES}}(\pi\nu)$  includes surface delta, spin–spin, and tensor interactions.

The Hamiltonian (1) was diagonalized in the proton–neutron–boson basis:  $|(j_\pi, j_\nu) j_{\pi\nu}, n_d I; J\rangle$ , where  $j_\pi$  and  $j_\nu$  stand for the proton and neutron angular momenta coupled to  $j_{\pi\nu}$ ,  $n_d$  is the number of  $d$  bosons,  $I$  is their angular momentum, and  $J$  is the spin of the state. The computer codes used in the calculations were written by Brant, Paar and Vretenar.<sup>29</sup>

## 4.2. Method of calculation. Parametrization

In the first stage of the calculations we fitted the  $\{h_i\}$  parameters of the  $H_{\text{IBM}}$  Hamiltonian (2) to the energy spectrum of the corresponding core nuclei ( $^{64}\text{Zn}$ ,  $^{66}\text{Zn}$ ,  $^{68}\text{Ge}$ ,  $^{70}\text{Ge}$ , and  $^{72}\text{Ge}$ ).

The total boson number is given by the number of valence shell pairs. For example, in  $^{66}\text{Zn}_{36}$  (the core of  $^{68}\text{Ga}_{37}$ ) we have  $N=5$ , since in this nucleus there are one proton and four neutron bosons, relative to the  $Z=N=28$  doubly magic nucleus. In the case of  $^{70}\text{Ge}_{38}$  (the core of  $^{72}\text{As}_{39}$ ) and  $^{71}\text{Ge}_{39}$  the calculations were performed with both  $N=7$  and  $N=4$ . The two calculations, with renormalization of the other parameters, gave similar results for the energy spectra and electromagnetic properties.<sup>9</sup> Thus, in the further calculations for  $^{70}\text{As}$ ,  $^{72}\text{As}$ ,  $^{74}\text{As}$ , and nine neighboring nuclei we have used reduced total boson numbers, by renormalizing the IBM pa-

TABLE II. Main components ( $\geq 4\%$ ) in the IBFFM wave functions of some low-lying states in  $^{66}\text{Ga}$ . The basis states are  $|(j_\pi j_\nu) j_{\pi\nu}, n_d I; J\rangle$  (see the text). The last column displays the corresponding amplitudes in the wave functions.

$J^\pi$	$(j_\pi, j_\nu)$	$j_{\pi\nu}; n_d I$	$A$	$J^\pi$	$(j_\pi, j_\nu)$	$j_{\pi\nu}; n_d I$	$A$
$0_1^+$	(3/2, 5/2)	2:12	0.62	$2_2^+$	(3/2, 5/2)	2:00	0.35
	(3/2, 3/2)	0:00	0.23		(3/2, 3/2)	2:00	0.45
	(3/2, 3/2)	2:12	0.43		(3/2, 5/2)	3:12	-0.24
	(1/2, 5/2)	2:12	-0.26	$0_2^+$	(3/2, 3/2)	3:12	-0.41
	(1/2, 3/2)	2:12	0.30		(3/2, 3/2)	0:00	0.36
$1_1^+$	(3/2, 5/2)	2:32	-0.22	$4_1^+$	(1/2, 1/2)	0:00	-0.25
	(3/2, 5/2)	1:00	0.54		(5/2, 5/2)	0:00	-0.53
	(3/2, 5/2)	1:20	-0.24		(5/2, 5/2)	0:20	0.28
	(3/2, 3/2)	2:12	0.31		(3/2, 5/2)	2:12	-0.43
	(1/2, 5/2)	2:12	0.24		(1/2, 3/2)	2:12	0.21
$2_1^+$	(3/2, 5/2)	3:12	0.41		(1/2, 5/2)	3:12	-0.21
	(3/2, 3/2)	3:12	-0.23	$5_1^-$	(3/2, 5/2)	4:00	0.62
	(3/2, 5/2)	2:00	0.62		(5/2, 5/2)	4:00	0.37
	(1/2, 5/2)	2:00	-0.25		(3/2, 5/2)	4:20	-0.26
	(3/2, 5/2)	2:12	-0.23		(5/2, 5/2)	5:12	0.39
$1_2^+$	(3/2, 5/2)	2:20	-0.27		(1/2, 9/2)	5:00	0.63
	(1/2, 5/2)	3:12	-0.27	$7_1^-$	(5/2, 9/2)	5:00	-0.38
	(5/2, 5/2)	4:12	-0.26		(1/2, 9/2)	5:20	-0.30
	(3/2, 5/2)	1:00	0.51		(5/2, 9/2)	7:12	0.35
	(3/2, 5/2)	1:20	-0.21		(1/2, 9/2)	5:12	0.32
$3_1^+$	(3/2, 5/2)	2:12	0.30		(5/2, 9/2)	7:00	0.74
	(3/2, 3/2)	2:12	-0.24		(5/2, 9/2)	7:12	-0.26
	(1/2, 3/2)	2:12	-0.26		(5/2, 9/2)	7:20	-0.39
	(3/2, 3/2)	3:12	0.33				
	(3/2, 5/2)	3:00	-0.46				
	(3/2, 3/2)	3:00	0.20				
	(1/2, 5/2)	3:00	0.50				
	(1/2, 5/2)	3:20	-0.23				
	(5/2, 5/2)	5:12	0.43				

rameters. This strongly reduced the volume of computations for odd-odd nuclei, without a substantial effect on the properties of the low-lying states.

The  $\chi$  and vibrational charge ( $e^{\text{vib}}$ ) parameters were fitted to the electromagnetic moments and reduced  $B(E2)$  transition probabilities of the core nuclei.

The nucleus  $^{66}\text{Zn}$  exhibits a level scheme which is characteristic of a spherical vibrator. In this case the parameters  $h_2$  and  $h_3$  were chosen to be equal to zero. In other nuclei we employed a parametrization which corresponds to a transition between the  $U(5)$  and  $O(6)$  dynamical symmetries, but somewhat closer to the  $U(5)$  character.

The core parameters employed in the calculations are given in the first part of Table I.

In the second stage of the calculations we adjusted the parameters of  $H_{\text{IBFM}}(\pi)$  [Eqs. (4)–(8)] to the experimental data of the corresponding odd- $Z$ , even- $N$  nuclei. The proton quasiparticle energies and occupation probabilities were

taken mostly from proton-transfer reaction data and/or pairing-force (BCS) calculations.

The  $A_0^\pi$  monopole,  $\Gamma_0^\pi$  dynamical quadrupole, and  $\Lambda_0^\pi$  exchange boson–fermion interaction strengths were fitted to the low-energy spectra of  $^{65}\text{Ga}$ ,  $^{67}\text{Ga}$ ,  $^{71}\text{As}$ , and  $^{73}\text{As}$ , respectively. (The level spectrum of  $^{69}\text{As}$  was scarcely known.) The effective gyromagnetic ratios  $g_s^\pi$  and  $g_{\text{tens}}^\pi$  were determined by fitting to the electromagnetic moments and reduced  $B(E2)$ ,  $B(M1)$  transition probabilities ( $\gamma$ -branching ratios).

In the third stage of the calculations we adjusted the parameters  $A_0^\nu$ ,  $\Gamma_0^\nu$ , and  $\Lambda_0^\nu$  of  $H_{\text{IBFM}}(\nu)$  [Eqs. (4)–(8)] to the low-energy spectra of the corresponding even- $Z$ , odd- $N$  nuclei:  $^{65}\text{Zn}$ ,  $^{67}\text{Zn}$ ,  $^{69}\text{Ge}$ ,  $^{71}\text{Ge}$ , and  $^{73}\text{Ge}$ . The proton quasiparticle energies and occupation probabilities were close to the calculated BCS values of Ref. 15 and to the systematics of the experimental data (Fig. 5). The parameters  $g_s^\nu$  and  $g_{\text{tens}}^\nu$  were fitted to the electromagnetic properties.

Finally, the parameters  $V_\delta$ ,  $V_{\sigma\sigma}$ , and  $V_{\text{tens}}$  of the residual

TABLE III. Wave functions of some low-lying states of  $^{70}\text{As}$ . Only the strongest components are given. The basis states are  $|(j_\pi j_\nu) j_\pi j_\nu, n_d I; J\rangle$  (see the text).

$J^\pi$	$(j_\pi, j_\nu)$	$j_\pi j_\nu, n_d I$	$ A $	$J^\pi$	$(j_\pi, j_\nu)$	$j_\pi j_\nu, n_d I$	$ A $
$0_1^+$	(5/2, 5/2)	0:00	0.83	$3_4^+$	(3/2, 5/2)	3:00	0.79
$0_2^+$	(1/2, 1/2)	0:00	0.70	$4_1^+$	(5/2, 5/2)	4:00	0.77
$1_1^+$	(3/2, 5/2)	1:00	0.73	$4_2^+$	(3/2, 5/2)	4:00	0.56
$1_2^+$	(5/2, 5/2)	1:00	0.66		(5/2, 5/2)	5:12	0.48
$1_3^+$	(1/2, 1/2)	1:00	0.66	$2_1^-$	(5/2, 9/2)	2:00	0.76
$2_1^+$	(5/2, 5/2)	2:00	0.51	$3_1^-$	(5/2, 9/2)	3:00	0.75
	(1/2, 5/2)	2:00	0.45	$4_1^-$	(1/2, 9/2)	4:00	0.52
$2_2^+$	(5/2, 5/2)	2:00	0.56		(5/2, 9/2)	4:00	0.41
	(3/2, 5/2)	2:00	0.41	$4_2^-$	(5/2, 9/2)	4:00	0.65
$2_3^+$	(5/2, 1/2)	2:00	0.63	$5_1^-$	(5/2, 9/2)	5:00	0.56
$3_1^+$	(1/2, 5/2)	3:00	0.51		(1/2, 9/2)	5:00	0.49
	(5/2, 5/2)	3:00	0.48	$6_1^-$	(5/2, 9/2)	6:00	0.70
$3_2^+$	(5/2, 5/2)	3:00	0.63	$7_1^-$	(5/2, 9/2)	7:00	0.75
$3_3^+$	(5/2, 1/2)	3:00	0.78				

interaction (10) were fitted to the experimental data on odd-odd nuclei. The core parameters and occupation probabilities remained unaltered in all cases. We remark that in  $^{70}\text{As}$ ,  $^{72}\text{As}$ , and  $^{74}\text{As}$  readjustment of the quasiparticle energies, boson-fermion interaction strengths, and effective gyromagnetic ratios was needed in order to obtain better agreement with the experimental data. Such a renormalization seems to be in accord with a general observation in the region of soft nuclei: the dynamical deformation can be sizable if one nucleon is added. Consequently, the parameters may change noticeably from those derived from the neighboring nuclides. A similar feature was found, for example, in the  $A=130$  region.

The parameters applied for the IBFFM description of the properties of the odd-odd nuclei are summarized in Table I.

#### 4.3. Results. Discussion

The calculated energy spectra are compared with the experimental data in Figs. 8 ( $^{64}\text{Zn}$ ,  $^{65}\text{Ga}$ ), 9 ( $^{65}\text{Zn}$ ,  $^{66}\text{Ga}$ ), 10 ( $^{66}\text{Zn}$ ,  $^{67}\text{Ga}$ ), 11 ( $^{67}\text{Zn}$ ,  $^{68}\text{Ga}$ ), 12 ( $^{68}\text{Ge}$ ,  $^{69}\text{Ge}$ ,  $^{70}\text{As}$ ), 13 ( $^{70}\text{Ge}$ ,  $^{71}\text{As}$ ), 14 ( $^{71}\text{Ge}$ ,  $^{72}\text{As}$ ), 15 ( $^{72}\text{Ge}$ ,  $^{73}\text{As}$ ), and 16 ( $^{73}\text{Ge}$ ,  $^{74}\text{As}$ ). Although the level schemes are usually very complicated (especially in odd-odd nuclei), reasonable agreement has been obtained between experiment and theory. The calculated states are usually assigned to the experimental levels on the basis of the energy, spin, parity, one-nucleon transfer reaction data (if they exist), decay properties, and wave functions.

The main components of the wave functions of some low-lying states in  $^{66}\text{Ga}$  and  $^{70}\text{As}$  are shown in Tables II and III, respectively. Usually, the wave functions are very complex. There are states which have more than 600 components. Nevertheless, in some cases the states are dominated

by only one proton-neutron multiplet. Thus, it is worth comparing the experimental and IBFFM energy spectra also with the predictions of the parabolic rule (Figs. 6 and 7).

*The  $\pi\tilde{p}_{3/2}\nu\tilde{f}_{5/2}$  multiplet.* As an example, let us discuss the energy splitting of the  $\pi\tilde{p}_{3/2}\nu\tilde{f}_{5/2}$  multiplet in  $^{66,68,70}\text{Ga}$  and  $^{70,72}\text{As}$ . The parabolic rule predicts an open-up parabola for the energy splitting in  $^{66}\text{Ga}$  and an open-down one in  $^{68}\text{Ga}$  (Fig. 7). This is in accord with the experimental facts, because the  $1^+$ ,  $2^+$ ,  $3^+$ , and  $4^+$  states of the multiplet can be identified with the 44- and 109-keV  $1_1^+ + 1_2^+$ , 66-keV  $2_1^+$ , 162-keV  $3_1^+$ , and 415-keV  $4_1^+$  states in  $^{66}\text{Ga}$  and 0-keV  $1_1^+$ , 175-keV  $2_1^+$ , 376- and 676-keV  $3_1^+ + 3_2^+$ , and 496-keV  $4_1^+$  states in  $^{68}\text{Ga}$  (Figs. 9 and 11). The IBFFM calculations are in accord with the classification of the parabolic rule, because the  $1_1^+ + 1_2^+$ ,  $2_1^+$ ,  $3_1^+$ , and  $4_1^+$  states in  $^{66}\text{Ga}$ , as well as the  $1_1^+$ ,  $2_1^+$ ,  $3_1^+ + 3_2^+$ , and  $4_1^+$  states in  $^{68}\text{Ga}$  have dominant (or at least very strong)  $\pi\tilde{p}_{3/2}\nu\tilde{f}_{5/2}$  components. The inversion of the parabola is connected with the fact that the  $\tilde{f}_{5/2}$  neutron is particle-like in  $^{66}\text{Ga}_{35}$  ( $V^2 < 0.5$ ) and hole-like in  $^{68}\text{Ga}_{37}$  ( $V^2 > 0.5$ ).

The  $\pi\tilde{p}_{3/2}\nu\tilde{f}_{5/2}$  multiplet is also seen in  $^{70}\text{Ga}$ , and the energy splitting exhibits an open-down parabola, in agreement with the prediction of the parabolic rule.<sup>7</sup>

The members of the  $\pi\tilde{p}_{3/2}\nu\tilde{f}_{5/2}$  multiplet in  $^{70}\text{As}$  are fragmented into different states. Nevertheless, in the  $1_1^+$ ,  $3_4^+$ , and  $4_2^+$  states the  $\pi\tilde{p}_{3/2}\nu\tilde{f}_{5/2}$  components are dominant (Table III).

On the basis of lifetime measurements and other considerations Hübner<sup>44</sup> came to the conclusion that the  $1_1^+$  state of  $^{72}\text{As}$  has either the  $\pi p_{3/2}^{-1}\nu f_{5/2}^{-1}$  or the  $\pi p_{3/2}^{-1}\nu p_{1/2}$  configuration. The IBFFM calculations give  $\pi\tilde{p}_{3/2}\nu\tilde{f}_{5/2}$  as the dominant configuration for this state. The parabolic rule predicts



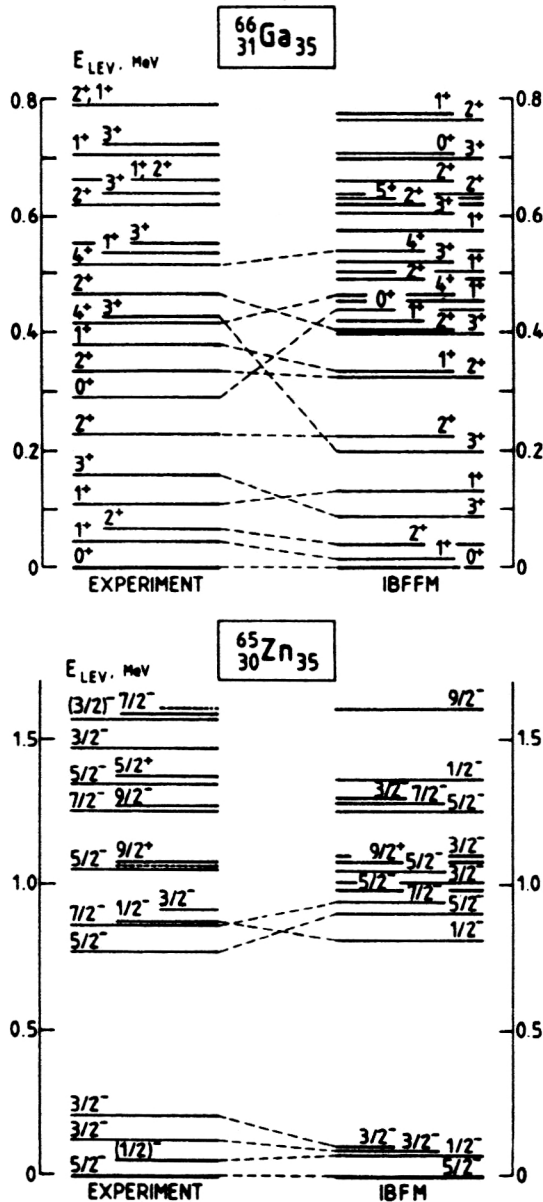


FIG. 9. Experimental energy spectra of  $^{66}\text{Zn}$  (Ref. 31) and  $^{66}\text{Ga}$  (Ref. 4) and the corresponding theoretical IBFM and IBFFM results.<sup>4</sup>

an open-down parabola for the energy splitting of the  $\pi\tilde{p}_{3/2}\nu\tilde{f}_{5/2}$  multiplet, with a minimum energy for the  $1^+$  state. The  $4^+$  member of this multiplet may be the  $4_1$  state. The  $2^+$  and  $3^+$  members are fragmented into different states (e.g.,  $2_1^+$ ,  $2_2^+$ , etc.; see Table IX in Ref. 9).

**The  $\pi\tilde{p}_{3/2}\nu\tilde{p}_{1/2}$  doublet.** In the case of doublets, for example, in  $\pi\tilde{p}_{3/2}\nu\tilde{p}_{1/2}$ , the energy splitting does not depend on the occupation probability, so that the shape of the splitting of the given multiplet is very similar for all investigated nuclei (see Fig. 7). The  $1^+$  and  $2^+$  members of the  $\pi\tilde{p}_{3/2}\nu\tilde{p}_{1/2}$  doublet are clearly seen in  $^{70}\text{Ga}$  (Ref. 7) and  $^{74}\text{As}$  (Ref. 11). In both cases  $E(1^+) < E(2^+)$ , in agreement with the predictions of the parabolic rule and IBFFM calculations (for  $^{74}\text{As}$ ; see the  $1_1^+$  and  $2_1^+$  states in Fig. 17).

Some members of the  $\pi\tilde{f}_{5/2}\nu\tilde{f}_{5/2}$  multiplet were identified in  $^{70}\text{As}$  and  $^{72}\text{As}$ .

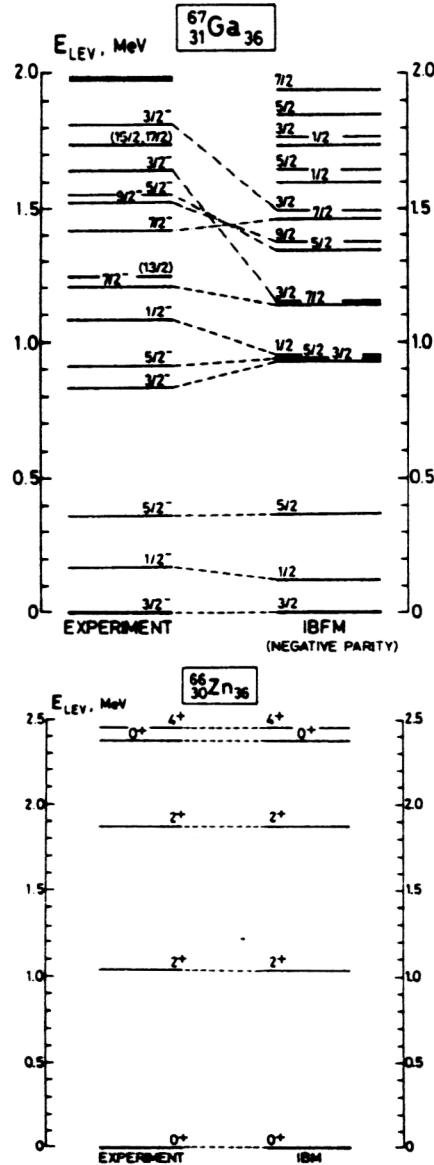


FIG. 10. Experimental energy spectra of  $^{67}\text{Zn}$  (Ref. 30) and  $^{67}\text{Ga}$  (Ref. 32) and the corresponding theoretical IBM and IBFM results.<sup>5,6</sup> The dashed lines show the assignment of the theoretical levels to the experimental ones. If the assignment is made on the basis of the energies only, it is marked by a dot-dash line.

According to the parabolic rule, the lowest-lying  $0^+$  states in  $^{70}\text{As}$  are expected to be relatively pure, and they belong to the  $\pi\tilde{f}_{5/2}\nu\tilde{f}_{5/2}$  and/or  $\pi\tilde{p}_{1/2}\nu\tilde{p}_{1/2}$  quasiparticle multiplets. Many low-lying  $1^+$  levels are expected, with a strong configuration mixing among them. The same is true for the  $2^+$  and  $3^+$  states. The lowest-lying  $4_1^+$  state belongs to the  $\pi\tilde{f}_{5/2}\nu\tilde{f}_{5/2}$  multiplet, and it is probably well separated from the  $4^+$  members of the  $\pi\tilde{p}_{3/2}\nu\tilde{f}_{5/2}$  and  $\pi\tilde{f}_{5/2}\nu\tilde{p}_{3/2}$  multiplets.

The IBFFM calculations (Fig. 12 and Table III) show that the  $0_1^+$  345-keV and  $4_1^+$  ground states of  $^{70}\text{As}$  have  $\pi\tilde{f}_{5/2}\nu\tilde{f}_{5/2}$  as dominant configurations. The  $\pi\tilde{f}_{5/2}\nu\tilde{f}_{5/2}$  components are fragmented in the  $1_1^+$ ,  $1_2^+$ ,  $2_1^+$ ,  $2_2^+$ ,  $3_1^+$ ,  $3_2^+$  states with other components. The  $0_1^+$  state decays by a strong  $M1$

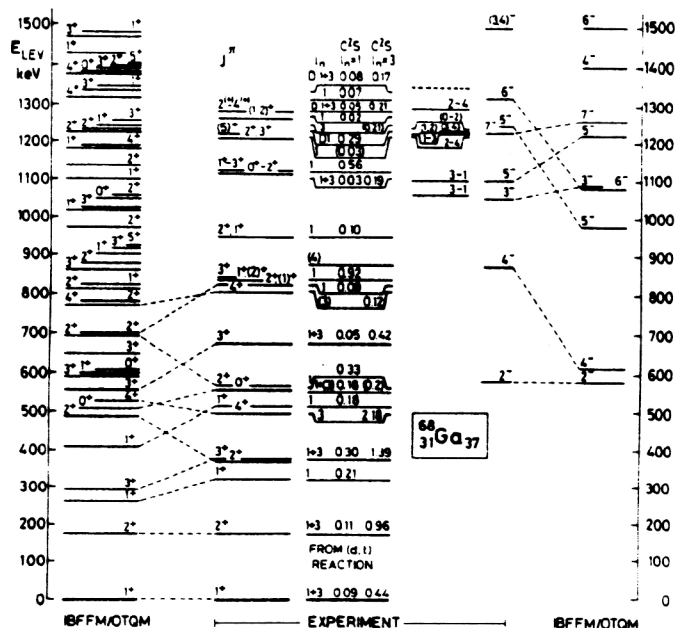


FIG. 11. Experimental energy spectra of  $^{67}\text{Zn}$  (Ref. 32) and  $^{68}\text{Ga}$  (Refs. 5 and 6) and the corresponding theoretical IBFM and IBFFM results.<sup>5,6</sup> The (d,t) reaction data are taken from Daehnack *et al.*<sup>33</sup> See also the caption to Fig. 10.

transition to the  $1_1^+$  state, as expected. The low-lying  $5^+$  member of the  $\pi\tilde{f}_{5/2}\nu\tilde{f}_{5/2}$  multiplet is missing in the experimental spectrum.

According to Bertschat *et al.*,<sup>45</sup> the best agreement between the predicted and measured  $g$  factors of the  $3_1^+$  state at 214 keV in  $^{72}\text{As}$  is obtained if one assumes the  $\pi\tilde{f}_{5/2}\nu\tilde{f}_{5/2}^{-1}$  and  $\pi\tilde{f}_{5/2}\nu p_{1/2}$  configurations. Our IBFFM calculations indicate a mixed configuration for this state, with the  $\pi\tilde{f}_{5/2}\nu\tilde{f}_{5/2}$  configuration as the strongest one. The parabolic rule predicts an open-up parabola for the splitting of the

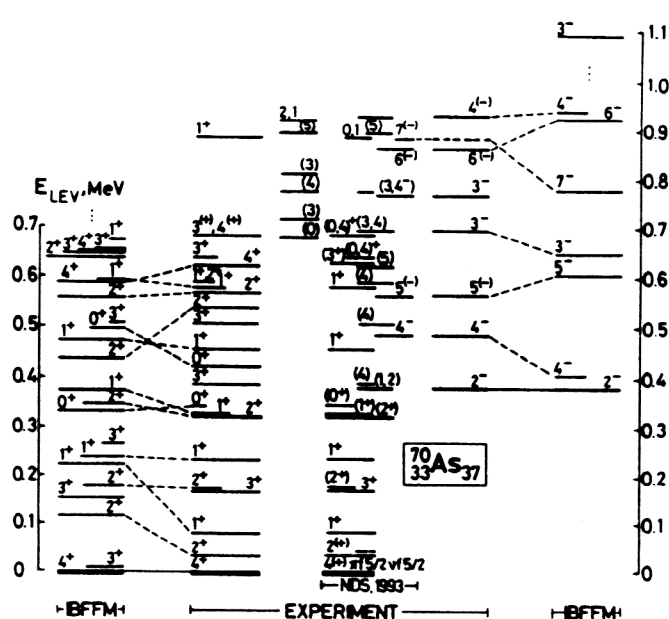


FIG. 12. Experimental energy spectra of  $^{68}\text{Ge}$  (Ref. 34),  $^{69}\text{Ge}$  (Ref. 35), and  $^{70}\text{As}$  (Refs. 8 and 36) and the corresponding theoretical IBM and IBFFM results.<sup>8</sup>

$\pi\tilde{f}_{5/2}\nu\tilde{f}_{5/2}$  multiplet, with a minimum energy for the  $3^+$  (or  $4^+$ ) member.

Some members of the  $\pi\tilde{f}_{5/2}\nu\tilde{g}_{9/2}$  multiplet were observed in almost all the investigated odd-odd Ga and As nuclei.

On the basis of the parabolic rule we may expect that the  $2_1^-$ ,  $3_1^-$ ,  $6_1^-$ , and  $7_1^-$  states in  $^{70}\text{As}$  are relatively pure and probably belong to the  $\pi\tilde{f}_{5/2}\nu\tilde{g}_{9/2}$  multiplet (see Fig. 6). In the low-lying  $4_1^-$  and  $5_1^-$  states there is probably a stronger configuration mixing. As Fig. 12 shows, the low-lying negative-parity states of  $^{70}\text{As}$  have been reasonably well reproduced by the IBFFM calculations. The  $2_1^-$ ,  $3_1^-$ ,  $6_1^-$ , and  $7_1^-$  levels are rather pure and belong mainly to the  $\pi\tilde{f}_{5/2}\nu\tilde{g}_{9/2}$  multiplet (Table III). The 699-keV  $3_1^-$  level decays by an  $M1$  transition to the  $2_1^-$  state, in accordance with expectations for the neighboring members of the same multiplet. The  $4_1^-$ ,  $4_2^-$ , and  $5_1^-$  states have mixed  $\pi\tilde{p}_{1/2}\nu\tilde{g}_{9/2}$  and

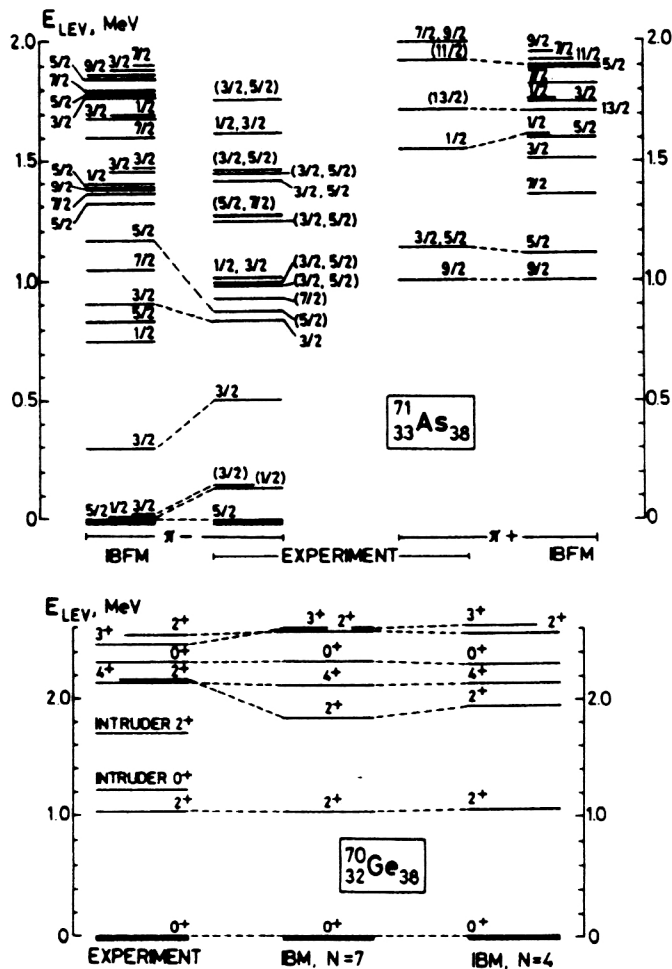


FIG. 13. Experimental energy spectra of  $^{70}\text{Ge}$  (Ref. 36) and  $^{71}\text{As}$  (Ref. 37) and the corresponding theoretical IBM and IBFM results.<sup>9,13</sup> The symbols  $\pi+$  and  $\pi-$  denote positive- and negative-parity states, respectively.

$\pi\tilde{f}_{5/2}\nu\tilde{g}_{9/2}$  multiplets as the main configurations.

According to the parabolic rule, the energy splitting of the  $\pi\tilde{f}_{5/2}\nu\tilde{g}_{9/2}$  multiplet shows an open-down parabola with a minimum energy for the  $2^-$  state in  $^{72}\text{As}$ . On the basis of a measurement of the magnetic dipole moment by Hogervorst *et al.*<sup>46</sup> one can conclude that the  $2^-$  ground state of  $^{72}\text{As}$  has predominantly a  $\pi\tilde{f}_{5/2}\nu\tilde{g}_{9/2}$  configuration. The IBFFM calculations confirm these results: in the  $2_1^-$  ground,  $3_1^-$ , and  $7_1^-$  states the dominant configuration is  $\pi\tilde{f}_{5/2}\nu\tilde{g}_{9/2}$  (Table IX in Ref. 9). In a recent publication Döring *et al.*<sup>47</sup> assigned to the 562.8-keV level values  $7^{(-)}$  for the spin and parity [instead of the former assignment (6)]. This state may be the  $7^-$  member of the  $\pi\tilde{f}_{5/2}\nu\tilde{g}_{9/2}$  multiplet (Fig. 14).

The  $2^-$  and  $7^-$  members of the  $\pi\tilde{f}_{5/2}\nu\tilde{g}_{9/2}$  multiplet could be identified also in  $^{68}\text{Ga}$  (Fig. 11 and Ref. 6) and  $^{70}\text{Ga}$  (Ref. 7); and the  $2^-$  member in  $^{74}\text{As}$  (Fig. 16 and Ref. 11).

The  $4^-$  and  $5^-$  members of the  $\pi\tilde{p}_{1/2}\nu\tilde{g}_{9/2}$  doublet were seen in  $^{68}\text{Ga}$  (Refs. 5 and 6),  $^{70}\text{As}$  (Ref. 8), and  $^{72}\text{As}$  (Ref. 9), although they are mixed with other components. According to the parabolic rule,  $E(4^-) < E(5^-)$  (see Figs. 6 and 7), in agreement with the experimental data and IBFFM calcula-

tions (Fig. 11 for  $^{68}\text{Ga}$ , Fig. 12 and Table III for  $^{70}\text{As}$ , and Fig. 14 and Table IX in Ref. 9 for  $^{72}\text{As}$ ).

In the low-lying  $5^-$  and  $6^-$  states, components of the  $\pi\tilde{p}_{3/2}\nu\tilde{g}_{9/2}$  multiplet were seen in  $^{68}\text{Ga}$  (Fig. 11 and Refs. 5 and 6) and  $^{70}\text{Ga}$  (Ref. 7).

The  $d$ -boson composition of the IBFFM wave functions of some low-lying states in  $^{66}\text{Ga}$  is given in Table IV. The  $0_1^+$  ground state of  $^{66}\text{Ga}$  is basically of one- $d$ -boson type. The total contribution of the sizable one- $d$ -boson components is 75%. We note that this is an effect of the boson-fermion interaction, similar to the  $j-1$  anomaly, which was studied previously in the cluster-vibration model for odd-even nuclei<sup>48</sup> and appears also in the IBFM for odd-even nuclei.<sup>24</sup>

The low-lying triplet of  $^{73}\text{Ge}$  positive-parity levels,  $9/2^+$ ,  $5/2^+$ , and  $7/2^+$  (see Fig. 16), is associated also with the  $J=j-1$ ,  $j-2$  anomaly due to lowering of the  $|\tilde{g}_{9/2,12;5/2}\rangle$  and  $|\tilde{g}_{9/2,12;7/2}\rangle$  one- $d$ -boson multiplet states. The  $5/2^+$  lowering is produced by the dynamical quadrupole interaction (and admixture of the  $d_{5/2}$  configuration from the shell above), while the  $7/2^+$  lowering is due to the exchange interaction.

The electromagnetic moments and the corresponding IB(FF)M results are given in Table V. Here we present calculated moments only for those states which have at least one experimentally measured moment (either electric quadrupole or magnetic dipole).

As Table V shows, the signs of the moments were correctly reproduced in 37 cases of the total of 39. (The exceptions are the electric quadrupole moments of the  $^{70}\text{As}$   $4_1^+$  and  $^{70}\text{Ge}$   $2_1^+$  states.) In 11 cases the signs of the moments were not determined experimentally. The calculations gave definite predictions for the signs, and allowed us to predict more than 200 moments which have so far not been measured (see Refs. 4, 9, and 11).

The calculated and available experimental  $B(E2)$ ,  $B(M1)$  reduced transition probabilities and  $\gamma$ -branching ratios for  $^{68}\text{Ga}$  transitions are given in Table VI. Similar data have been obtained also for  $^{66}\text{Ga}$  (Ref. 4),  $^{72}\text{As}$  (Ref. 9), and  $^{74}\text{As}$  (Ref. 11) transitions. As Table VI shows, there is reasonable agreement between the theory and experiment; at least all the leading branches are correctly reproduced. The  $\gamma$ -transition probabilities depend critically even on weak components of the wave function; we note a disagreement for the  $3_1^+ \rightarrow 1_1^+$  transition.

In Table VII we present the experimental and calculated spectroscopic factors for the  $(d,t)$  transfer reaction populating the low-lying levels in  $^{68}\text{Ga}$ .<sup>6</sup> Four levels (the  $1_1^+$ ,  $2_1^+$ ,  $2_2^+ + 3_1^+$ , and  $4_1^+$  states) are excited with large spectroscopic factors. According to the calculation, the low-lying  $1_1^+$ ,  $2_1^+$ ,  $3_1^+$ , and  $4_1^+$  states have the largest spectroscopic factors, in qualitative agreement with experiment. We have also calculated spectroscopic factors for the  $^{75}\text{As}(p,d)^{74}\text{As}$  and  $^{73}\text{Ge}(^3\text{He},d)^{74}\text{As}$  reactions.<sup>11</sup>

Summarizing the results, we have described the energy spectra and electromagnetic properties of even-even core isotopes, odd- $A$  neighbors, and odd-odd nuclei in a consistent way. For example, in the  $^{64}\text{Zn}$ ,  $^{65}\text{Zn}$ ,  $^{65}\text{Ga}$ , and  $^{66}\text{Ga}$  quartet more than 400 nuclear data (energy levels, moments, reduced transition probabilities,  $\gamma$ -branching ratios, etc.) have been calculated, using  $\leq 25$  (more or less freely fitted)

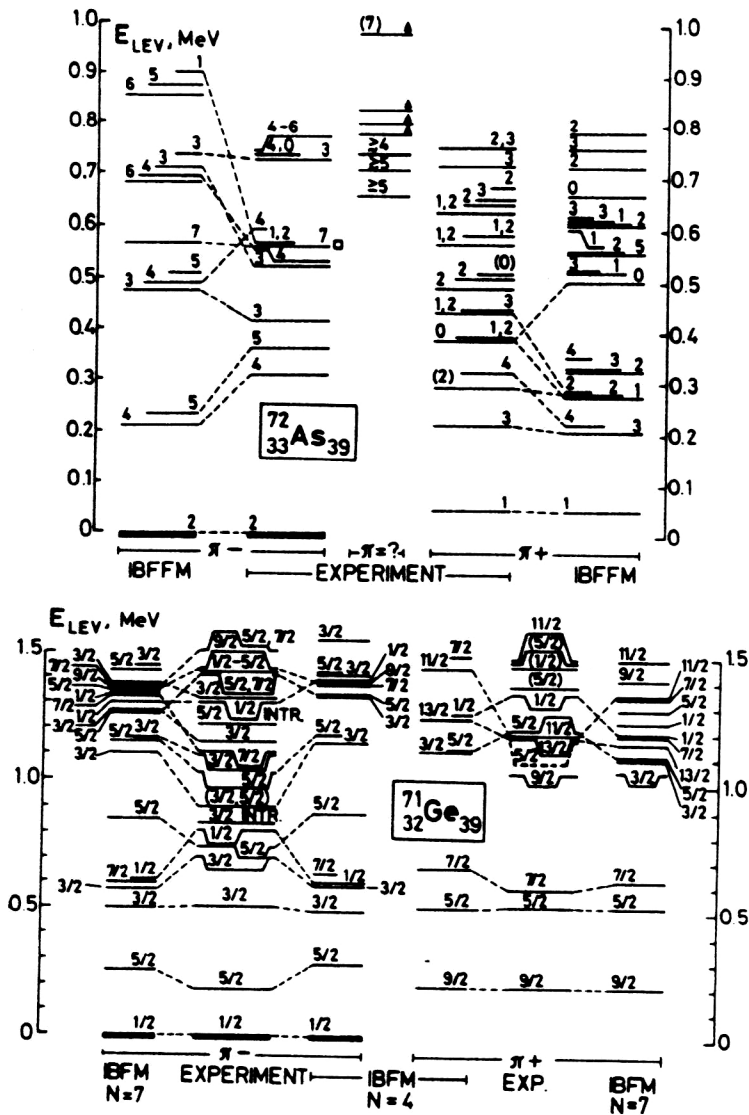


FIG. 14. Experimental energy spectra of  $^{71}\text{Ge}$  (Ref. 37) and  $^{72}\text{As}$  (Refs. 9 and 13) and the corresponding theoretical IBFM and IBFFM results.<sup>9,13</sup> The  $^{72}\text{As}$  levels, marked with  $\triangle$  and  $\square$ , were taken from the  $(\alpha, xnp)$  work of Mariscotti *et al.*<sup>38</sup> and Döring *et al.*,<sup>47</sup> respectively.

TABLE IV. The  $d$ -boson composition of the IBFFM wave functions of some low-lying states in  $^{66}\text{Ga}$ .

$J_k^\pi$	$n_d$				
	0	1	2	3	4
$0_1^+$	0.065	0.750	0.072	0.110	0.003
$1_1^+$	0.344	0.466	0.121	0.065	0.004
$2_1^+$	0.502	0.282	0.172	0.038	0.006
$1_2^+$	0.339	0.460	0.132	0.064	0.005
$3_1^+$	0.504	0.303	0.146	0.043	0.004
$2_2^+$	0.381	0.396	0.163	0.054	0.006
$0_2^+$	0.473	0.313	0.168	0.040	0.006

For each state  $J_k^\pi$ , the numbers in the table give the value of  $\sum_{j_\pi j_\nu} \xi^2[(j_\pi j_\nu) j_{\pi\nu}, n_d I; J]$  for each of the possible values of the  $d$ -boson number:  $n_d = 0, 1, 2, \dots, N$ .



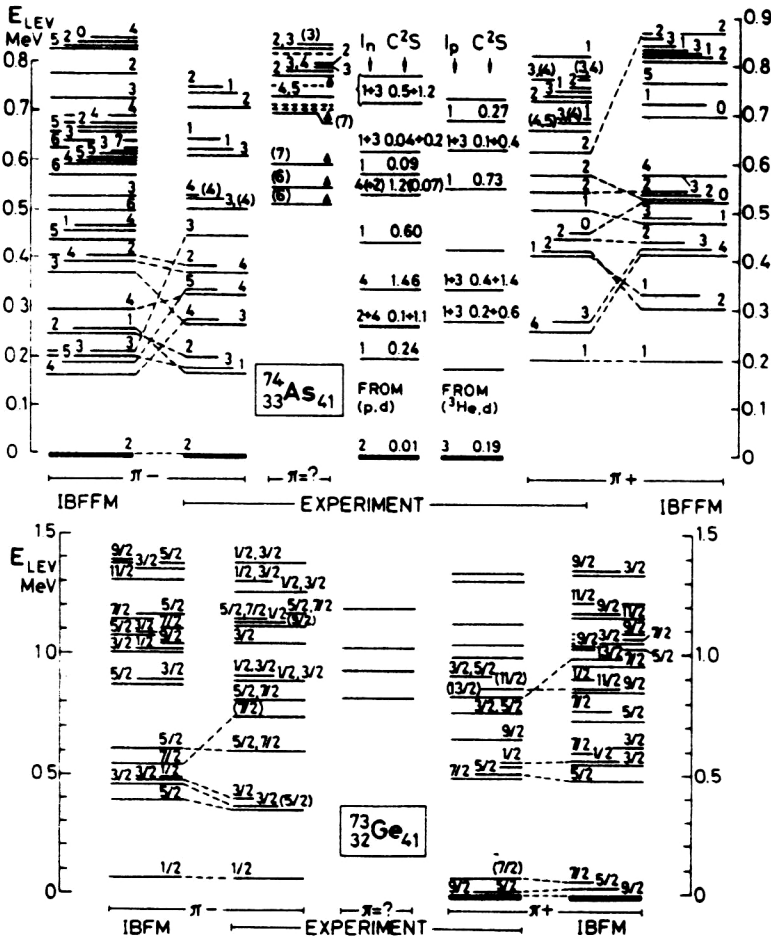


FIG. 16. Experimental energy spectra of  $^{73}\text{Ge}$  (Ref. 40) and  $^{74}\text{As}$  (Refs. 11 and 13) and the corresponding theoretical IBFM and IBFFM results.<sup>11,13</sup> The  $^{74}\text{As}$  levels, marked with  $\Delta$ , were taken from García Bermúdez *et al.*;<sup>41</sup> the  $(p,d)$  and  $(^3\text{He},d)$  results are from Fournier *et al.*<sup>42</sup> and Rosner *et al.*,<sup>43</sup> respectively.

nuclear moments and reduced transition probabilities have been calculated for the first time in our work.<sup>9,11</sup>

## 5. SUPERSYMMETRY IN $^{74}\text{Se}$ , $^{75}\text{Se}$ , $^{73}\text{As}$ , AND $^{74}\text{As}$ NUCLEI

On the basis of the vibrational-symmetry limit of the interacting boson-fermion model, Vervier *et al.*,<sup>53</sup> Čule and Paar,<sup>54</sup> and Van Isacker and Jolie<sup>55</sup> have developed formulas for the description of the level schemes of nuclei around  $^{76}\text{As}$ .

The new, more complete level schemes of  $^{74}\text{As}$  and  $^{73}\text{As}$  obtained in our work<sup>11</sup> offered a new possibility of checking the validity of the supersymmetry scheme. According to this scheme, the energy spectra of four nuclei (in the present case  $^{74}\text{Se}$ ,  $^{75}\text{Se}$ ,  $^{73}\text{As}$ , and  $^{74}\text{As}$ ) are interrelated and are described by the same Hamiltonian. The main advantage of this symmetry-based approximation is that the eigenvalue problem can be solved analytically.

According to Van Isacker and Jolie,<sup>55</sup> the eigenvalues of the Hamiltonian, the energies of the excited states, are given by the formula

$$\begin{aligned}
 E = & A_{\pi\nu} \sum_i N_i(N_i + 7 - 2i) + A_{\pi} \sum_i N_{i\pi}(N_{i\pi} + 7 - 2i) \\
 & + A_{\nu} \sum_i N_{i\nu}(N_{i\nu} + 7 - 2i) + B_1 \sum_i n_i + B_2 \sum_i n_i \\
 & \times (n_i + 6 - 2i) + C[v_1(v_1 + 3) + v_2(v_2 + 1)] \\
 & + DL(L + 1) + ES(S + 1) + FJ(J + 1), \quad (11)
 \end{aligned}$$

where  $N_i, N_{i\pi}, N_{i\nu}, n_i, v_1, v_2, L, S, J$  are quantum numbers and  $A_{\pi\nu}, A_{\pi}, A_{\nu}, B_1, B_2, C, D, E, F$  are parameters, which are not determined by the symmetry. The formula (11) was obtained for the  $U(5)$  limit of the  $U_{\pi}(6/12) \otimes U_{\nu}(6/12)$  supersymmetry (SUSY) (proton particle, neutron hole case and  $[N_i] \neq [N + 1, 1^5]$ ). (A somewhat different formula has been derived for  $[N_i] = [N + 1, 1^5]$ , but only a few levels belong to this group representation below 600 keV.)

First, we fitted the parameters of Eq. (11) to the levels of the even-even  $^{74}\text{Se}$ , odd- $A$   $^{75}\text{Se}$ , and  $^{73}\text{As}$  nuclei by a least-squares method. Quantum numbers were assigned to the states of the supermultiplet on the basis of the energies, spins, parities, decay properties, available one-nucleon transfer-reaction spectroscopic factors, as well as the IBF(F)M and SUSY wave functions of the levels considered. The following parameters were obtained  $A_{\pi} + A_{\pi\nu} = 55$ ,  $A_{\nu} + A_{\pi\nu} = 26$ ,  $B_1 = 525$ ,  $B_2 = 0$ ,  $C = 4$ ,  $D = -28$ , a high negative value for  $E$ , and  $F = 41$  (all in keV). Then we used these



TABLE V. Experimental electric quadrupole ( $Q$ ) and magnetic-dipole ( $\mu$ ) moments of Zn, Ga, Ge, and As nuclei compared with IB(FF)M theoretical results.

Nucleus	$J^\pi$	$E$ , keV	$Q(\text{eb})$		$\mu(\mu_N)$			Main config.
			Exp. [49]	Calc. Ref.	Exp. [49]	Calc.	Ref.	
$^{64}_{30}\text{Zn}_{34}$	$2^+_1$	992	-0.124(12) -0.143(21)	-0.07	+0.84(18) +0.92(20)	+0.94		One $d$ -boson
$^{65}_{30}\text{Zn}_{35}$	$5/2^-_1$	0	-0.023(2) <sup>u</sup>	-0.003	+0.769(2)	a)+1.38 b)+0.84		$\nu \bar{f} 5/2$
	$3/2^-_1$	115		+0.10	-0.78(20)	a)-1.49 b)-0.82		$\nu \bar{p} 3/2$
	$3/2^-_2$	207		-0.06 [4]	+0.73(25)	a)+0.52 b)+0.43 [4]		$\nu \bar{f} 5/2 \otimes 2^+$
	$9/2^+_1$	1066			-1.73(49)	a)-1.80 b)-1.03		$\nu \bar{g} 9/2$
$^{66}_{31}\text{Ga}_{35}$	$2^+_1$	66		-0.15	$\pm 1.011(18)^h$	a)+1.03 b)+0.72		$\pi \bar{p} 3/2 \nu \bar{f} 5/2$
	$7^-_1$	1464	$\pm 0.78(4)^{u, st}$	-0.40	+0.903(21)	a)-0.06 b)+0.70		$\pi \bar{f} 5/2 \nu \bar{g} 9/2$
	$9^+_1$	3043		-0.35	$\pm 4.23(90)$	a)+5.12 b)+4.59		
$^{66}_{30}\text{Zn}_{36}$	$2^+_1$	1039		-0.064	+0.94(22)	+0.91		One $d$ -boson
$^{67}_{30}\text{Zn}_{37}$	$5/2^-_1$	0	+0.150(15) <sup>u</sup>	+0.07	+0.8754790(84)	+1.35		$\nu \bar{f} 5/2$
	$1/2^-_1$	93			+0.587(11)	+0.72		$\nu \bar{p} 1/2$
	$3/2^-_1$	185		-0.04 [6]	+0.50(6)	+0.13 [6]		$\nu \bar{f} 5/2 \otimes 2^+$
	$9/2^+_1$	604	$\approx \pm 0.3(32)$	-0.20	-1.097(9)	-1.02		$\nu \bar{g} 9/2$
$^{67}_{31}\text{Ga}_{36}$	$3/2^-_1$	0	$\pm 0.195^{u, st}$	+0.07	+1.8507(3)	+2.08		$\pi \bar{p} 3/2$
$^{68}_{31}\text{Ga}_{37}$	$1^+_1$	0	$\pm 0.0277(14)^{k, st}$	+0.0082	$\pm 0.01175(5)^k$	-0.0134		$\pi \bar{p} 3/2 \nu \bar{f} 5/2$
	$7^-_1$	1230	$\pm 0.72(2)^{u, st}$	-0.514	+0.707(14)	+0.67		$\pi \bar{f} 5/2 \nu \bar{g} 9/2$
$^{69}_{32}\text{Ge}_{37}$	$5/2^-_1$	0	$\pm 0.024(5)^{u, st}$	+0.04	$\pm 0.735(7)$	0.73		$\nu \bar{f} 5/2$
$^{70}_{33}\text{As}_{37}$	$4^+_1$	0	+0.094(24)	-0.023 [8]	+2.1061(2)	+2.1 [8]		$\pi \bar{f} 5/2 \nu \bar{f} 5/2$
	$7^-_1$	888			+0.75(5) [50]	+0.77		$\pi \bar{f} 5/2 \nu \bar{g} 9/2$
$^{70}_{32}\text{Ge}_{38}$	$2^+_1$	1039	+0.03(6) or +0.09(6)	-0.197	+0.936(52)	+0.914		One $d$ -boson
$^{71}_{32}\text{Ge}_{39}$	$1/2^-_1$	0			+0.547(5)	+0.445		$\nu \bar{p} 1/2$
	$5/2^-_1$	175			+1.018(10)	+0.987		$\nu \bar{f} 5/2$
	$9/2^+_1$	199	$\pm 0.34(5)$	-0.230 [9]	-1.0413(7)	-1.221 [9]		$\nu \bar{g} 9/2$
$^{71}_{33}\text{As}_{38}$	$5/2^-_1$	0	-0.021(6)	-0.156	(+1.6735(18)	+1.010		$\pi \bar{f} 5/2$
	$9/2^+_1$	1001		-0.365	+5.15(9)	+5.985		$\pi \bar{g} 9/2$
$^{72}_{33}\text{As}_{39}$	$2^-_1$	0	-0.082(24)	-0.132	-2.1566(3)	-1.809		$\pi \bar{f} 5/2 \nu \bar{g} 9/2$
	$3^+_1$	214		+0.229	+1.580(18) <sup>h</sup>	+1.525		$\pi \bar{f} 5/2 \nu \bar{f} 5/2$
$^{72}_{32}\text{Ge}_{40}$	$2^+_1$	834	-0.13(6)	-0.209	+0.798(66)	+0.888		One $d$ -boson
$^{73}_{32}\text{Ge}_{41}$	$9/2^+_1$	0	-0.173(26) <sup>u</sup>	-0.165	-0.879467(12)	-1.204		$\nu \bar{g} 9/2$
	$5/2^-_1$	13	-0.4(3) or +0.22 [58]	+0.230	-0.0941(25)	-1.091		
$^{73}_{33}\text{As}_{40}$	$5/2^-_1$	67		-0.112 [11]	+1.63(10)	+0.964 [11]		$\pi \bar{f} 5/2$
	$9/2^+_1$	428		-0.392	+5.234(14)	+5.955		$\pi \bar{g} 9/2$
$^{74}_{33}\text{As}_{41}$	$2^-_1$	0		+0.111	-1.597(3)	-1.393		$\pi \bar{f} 5/2 \nu \bar{g} 9/2$
	$4^+_1$	259		+0.417	+3.238(40)	+3.793		$\pi \bar{p} 3/2 \nu \bar{f} 5/2$

a)  $g_s^p = 0.9 g_s^p$  (free); b)  $g_s^p = 0.5 g_s^p$  (free). h) Does not include Knight-shift correction.  
 $k) \mu/Q < 0$  (signs of  $\mu$  and  $Q$  are different). st) "Steinheimer" or other polarization correction included. u) No polarization correction included.

TABLE VI. Calculated  $E2$  and  $M1$  transitions between the low-lying levels in  $^{68}\text{Ga}$  and comparison with available data. The assignment of calculated to experimental levels is made according to Fig. 11.

$J_i^\pi \rightarrow J_f^\pi$	$10^2 B(E2) (e^2 b^2)$		$10 B(M1) (\mu_N^2)$		$I_\gamma$	
	IBFFM	Exp. [34]	IBFFM	Exp. [34]	IBFFM	Exp. [34]
$2_1^+ \rightarrow 1_1^+$	0.13		1.822	$\geq 0.014$	100	100
$1_2^+ \rightarrow 2_1^+$	0.03		0.130		5.5	5.5
$\rightarrow 1_1^+$	0.04		0.221		100	100
$2_2^+ \rightarrow 1_2^+$	0.25		0.024		0.1	
$\rightarrow 2_1^+$	0.002		0.044		11.9	3.0
$\rightarrow 1_1^+$	0.00006		0.056		100	100
$3_1^+ \rightarrow 2_2^+$	0.01		0.008		$10^{-7}$	
$\rightarrow 1_2^+$	0.0004				$10^{-7}$	
$\rightarrow 2_1^+$	0.44		1.593	$\geq 0.005$	100	100
$\rightarrow 1_1^+$	0.03	$\geq 0.05$			0.1	45
$4_1^+ \rightarrow 3_1^+$	0.40		1.389	$\geq 0.038$	100	100
$\rightarrow 2_2^+$	0.01				0.0008	
$\rightarrow 2_1^+$	0.03	$> 0.01$			0.3	4.6
$1_3^+ \rightarrow 3_1^+$	0.09				0.006	
$\rightarrow 2_2^+$	0.48		0.050		2.6	4.2
$\rightarrow 1_2^+$	0.23		0.036		5.0	1.0
$\rightarrow 2_1^+$	0.03		0.134		100	100
$\rightarrow 1_1^+$	0.002		0.004		10.5	20
$0_1^+ \rightarrow 1_3^+$			0.217		0.08	
$\rightarrow 2_2^+$	0.02				0.001	
$\rightarrow 1_2^+$			0.925		60	15
$\rightarrow 2_1^+$	1.01				2.8	
$\rightarrow 1_1^+$			0.116		100	100
$2_3^+ \rightarrow 0_1^+$	0.00007				$3 \times 10^{-12}$	
$\rightarrow 1_3^+$	0.08		0.009		0.01	
$\rightarrow 4_1^+$	0.004				$5 \times 10^{-6}$	
$\rightarrow 3_1^+$	0.23		0.271		21	0.9
$\rightarrow 2_2^+$	0.04		0.444		35	5.0
$\rightarrow 1_2^+$	0.005		0.050		8.3	5.8
$\rightarrow 2_1^+$	1.34		0.0003		9.8	13.4
$\rightarrow 1_1^+$	0.20		0.044		100	100
$3_2^+ \rightarrow 2_3^+$	0.12		0.377		0.7	
$\rightarrow 1_3^+$	0.25				0.003	
$\rightarrow 4_1^+$	0.22		0.00002		0.004	
$\rightarrow 3_1^+$	0.19		0.0003		0.1	9.3
$\rightarrow 2_2^+$	0.05		0.065		2.5	
$\rightarrow 1_2^+$	0.09				0.05	
$\rightarrow 2_1^+$	0.19		0.561		100	100
$\rightarrow 1_1^+$	0.04				0.6	2.8
$4_2^+ \rightarrow 3_2^+$	1.06		0.167		2.1	
$\rightarrow 2_3^+$	0.01				0.003	
$\rightarrow 4_1^+$	0.06		0.583	$\geq 0.0014$	100	100
$\rightarrow 3_1^+$	0.58		0.257	$\geq 0.0004$	121	90
$\rightarrow 2_2^+$	0.02				0.1	
$\rightarrow 2_1^+$	0.60				24	20

TABLE VI. (Continued.)

TABLE VI. (Continued.)

$J_i^{\pi} \rightarrow J_f^{\pi}$	$10^2 B(E2) (e^2 b^2)$		$10 B(M1) (\mu_N^2)$		$I_{\gamma}$	
IBFFM	IBFFM	Exp. [34]	IBFFM	Exp. [34]	IBFFM	Exp. [34]
$2_4^+ \rightarrow 4_2^+$	0.32				$4 \times 10^{-8}$	
$\rightarrow 3_2^+$	0.03		0.009		0.02	
$\rightarrow 2_3^+$	0.26		0.062		0.6	2.4
$\rightarrow 0_1^+$	0.001				0.00005	
$\rightarrow 1_3^+$	0.12		0.034		0.6	
$\rightarrow 4_1^+$	0.21				0.03	
$\rightarrow 3_1^+$	0.66		0.029		1.9	8.6
$\rightarrow 2_2^+$	0.002		0.013		0.6	4.6
$\rightarrow 1_2^+$	0.006		0.032		2.2	10.5
$\rightarrow 2_1^+$	0.0003		0.026		3.8	4.7
$\rightarrow 1_1^+$	0.93		0.291		100	100
$4_1^- \rightarrow 2_1^-$	2.69	$\geq 0.21$			100	100
$3_1^- \rightarrow 4_1^-$	1.01		1.212		1.1	
$\rightarrow 2_1^-$	2.10		5.934		100	100
$5_2^- \rightarrow 3_1^-$	0.004				$10^{-6}$	
$\rightarrow 4_1^-$	0.19		0.579		100	100
$7_1^- \rightarrow 5_2^-$	0.21				100	100
$5_1^- \rightarrow 7_1^-$	4.27				$10^{-6}$	
$\rightarrow 5_2^-$	0.18		0.304		1.2	
$\rightarrow 3_1^-$	1.36				0.03	
$\rightarrow 4_1^-$	0.32		1.533		100	100
$6_1^- \rightarrow 5_1^-$	0.04		0.072		0.06	$\leq 17$
$\rightarrow 7_1^-$	0.02		0.076		0.1	
$\rightarrow 5_2^-$	0.47		5.019		100	100
$\rightarrow 4_1^-$	0.96				2.2	8

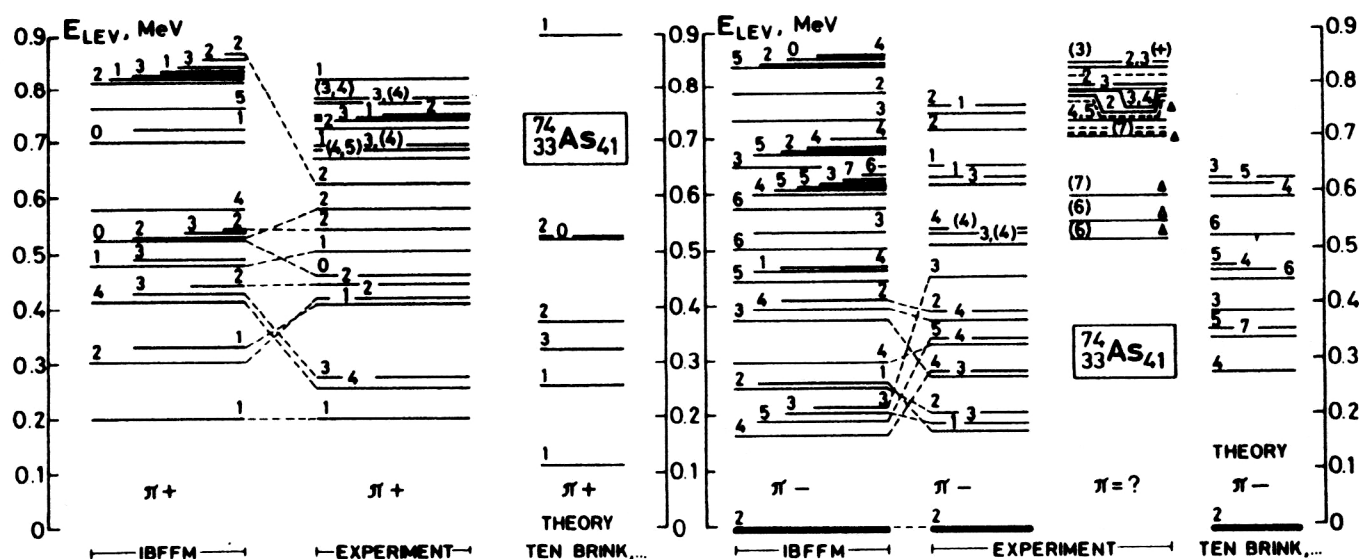


FIG. 17. Level scheme of  $^{74}\text{As}$  (Ref. 11), compared with the present IBFFM and previous calculations by Ten Brink *et al.*<sup>51</sup> The levels marked with triangles were observed in Ref. 41 from the  $(\alpha, np\gamma)$  reaction.

TABLE VII. Spectroscopic factors for the  $^{69}\text{Ga}_{38}(d,t)^{68}\text{Ga}_{37}$  transfer reaction populating the low-lying levels in  $^{68}\text{Ga}$ .

$J^\pi$	$C^2S$						
	IBFM				Exp [33]		
IBFM	$P_{1/2}$	$P_{3/2}$	$f_{5/2}$	$g_{9/2}$	$P_{1/2} + P_{3/2}$	$f_{5/2}$	$g_{9/2}$
$1_1^+$	0.012	0.003	3.333		0.09	0.44	
$2_1^+$	0.023	0.002	3.230		0.11	0.96	
$1_2^+$	0.308	0.015	0.170		0.21		
$2_2^+$	0.344	0.430	0.063		0.30	1.39	
$3_1^+$		0.114	2.772				
$4_1^+$			3.227			2.18	
$1_3^+$	0.055	0.283	0.032		0.18		
$0_1^+$		0.403			0.18	0.2	
$2_3^+$	0.004	0.210	0.007		0.33		
$3_2^+$		1.050	0.278		0.05	0.42	
$4_2^+$			0.438			0.12	
$2_4^+$	0.005	0.0004	0.178		0.09		
$4_1^-$				0.094			
$3_1^-$				0.020			
$5_2^-$				0.476			
$5_1^-$				0.003			
$6_1^-$				0.360			

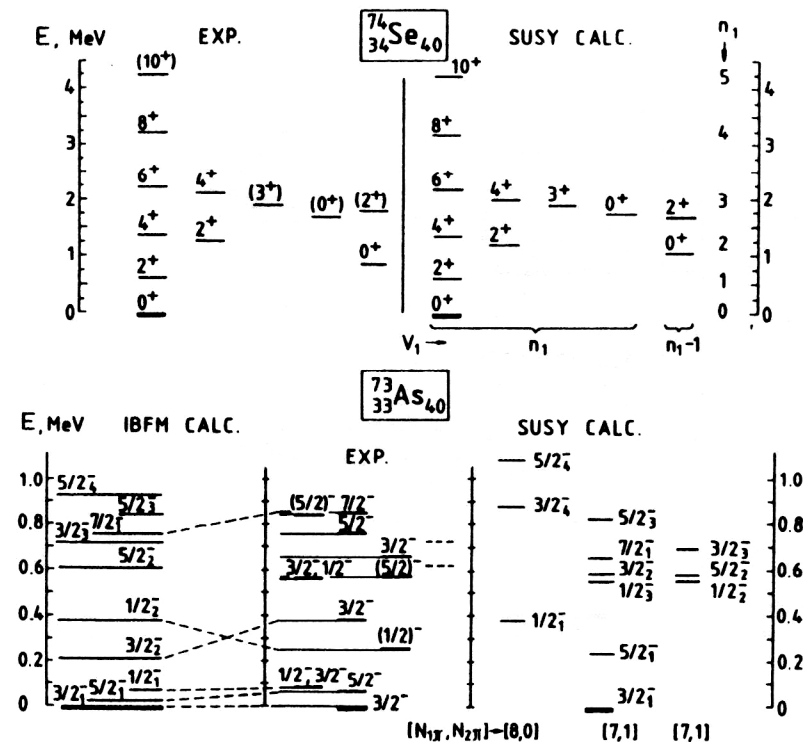


FIG. 18. Upper part: experimental energy levels of  $^{74}\text{Se}$  (Ref. 56) in comparison with the SUSY calculations. Lower part: experimental energy levels of  $^{73}\text{As}$  (Refs. 10 and 40) in comparison with the IBFM and SUSY calculations.

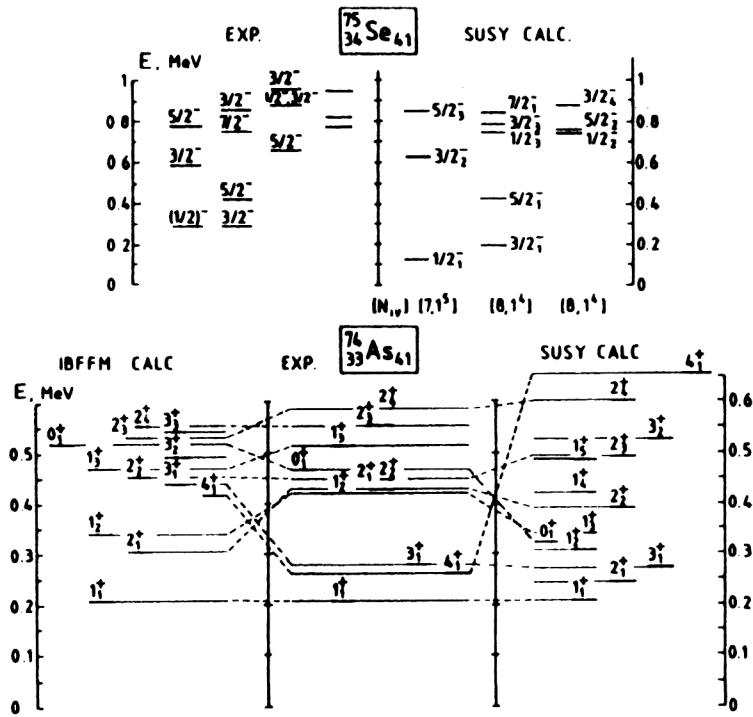


FIG. 19. Upper part: experimental energy levels of  $^{75}\text{Se}$  (Ref. 57) in comparison with the SUSY calculations. Lower part: experimental energy levels of  $^{74}\text{As}$  (Ref. 11) in comparison with the IBFFM<sup>11</sup> and SUSY<sup>12</sup> calculations. If the assignment of calculated levels to experimental ones is made on the basis of the energies only, it is marked with a dot-dash line.

parameters to generate the level spectrum of  $^{74}\text{As}$ . (The value of  $A_{\pi\nu}$  was taken as zero, after testing its role in the generated  $^{74}\text{As}$  spectrum.)

The experimental and calculated energy spectra are compared in Figs. 18 and 19.

The supersymmetry calculations describe 44 levels of four different nuclei reasonably well with only seven fitted parameters. However, a problem appears with additional  $1^+$  and  $3^+$  states in the low-energy SUSY spectrum, and the assignment of some SUSY states to experimental ones cannot be made unambiguously.

The supersymmetry calculations and results are described in detail in Ref. 12.

We are indebted to all co-authors of Refs. 4–14 for effective collaboration. The financial support of the Hungarian National Scientific Foundation (OTKA, grant No. 3004) is gratefully acknowledged.

<sup>11</sup> A. Algara, D. Sohler, T. Fényes, Z. Gácsi, S. Brant, and V. Paar, Preprint, Inst. Nucl. Res. (ATOMKI), Debrecen, 3-1994-P; and to be published.

<sup>12</sup> A. Algara, T. Fényes, Zs. Dombrádi, and J. Jolie, Preprint, Inst. Nucl. Res. (ATOMKI), Debrecen, 6-1994-P; and to be published.

<sup>13</sup> T. Fényes, A. Algara, Zs. Podolyák, D. Sohler, J. Timár, V. Paar, S. Brant, and Lj. Šimić, Proc. Int. Conf. on Perspectives for the Interacting Boson Model, Padova, 1994 (World Scientific, Singapore, 1994); in press.

<sup>14</sup> Z. Gácsi, J. Gulyás, T. Kibédi, E. Koltay, A. Krasznahorkay, and T. Fényes, Izv. Akad. Nauk SSSR, Ser. Fiz. **47**, 45 (1983).

<sup>15</sup> R. Fournier, J. Kroon, T. H. Hsu, B. Hird, and G. C. Ball, Nucl. Phys. **A202**, 1 (1973).

<sup>16</sup> V. Paar, Nucl. Phys. **A331**, 16 (1979).

<sup>17</sup> V. Paar, in *In-Beam Nuclear Spectroscopy*, Vol. 2, edited by Zs. Dombrádi and T. Fényes (Akad. Kiadó, Budapest, 1984), p. 675; in *Capture Gamma-Ray Spectroscopy*, AIP Conf. Proc. 125 (AIP, New York, 1985), p. 70.

<sup>18</sup> S. Brant, V. Paar, and D. Vretenar, Z. Phys. A **319**, 351 (1984); V. Paar, D. K. Sunko, and D. Vretenar, Z. Phys. A **327**, 291 (1987).

<sup>19</sup> T. Kibédi, Zs. Dombrádi, T. Fényes, A. Krasznahorkay, J. Timár, Z. Gácsi, A. Passoja, V. Paar, and D. Vretenar, Phys. Rev. C **37**, 2391 (1988); Z. Gácsi, Zs. Dombrádi, T. Fényes, S. Brant, and V. Paar, Phys. Rev. C **44**, 642 (1991).

<sup>20</sup> V. Lopac, S. Brant, V. Paar, O. W. B. Schult, H. Seyfarth, and A. B. Balantekin, Z. Phys. A **323**, 491 (1986).

<sup>21</sup> A. Arima and F. Iachello, Phys. Rev. Lett. **35**, 157 (1975); Ann. Phys. (N.Y.) **99**, 253 (1976); **111**, 201 (1978); **123**, 468 (1979).

<sup>22</sup> F. Iachello and A. Arima, *The Interacting Boson Model* (Cambridge University Press, Cambridge, 1987).

<sup>23</sup> F. Iachello and O. Scholten, Phys. Rev. Lett. **43**, 679 (1979).

<sup>24</sup> O. Scholten, Prog. Part. Nucl. Phys. **14**, 189 (1985); Ph.D. Thesis, University of Groningen (1980).

<sup>25</sup> D. Bonatsos, *Interacting Boson Models of Nuclear Structure* (Clarendon Press, Oxford, 1988).

<sup>26</sup> D. Janssen, R. V. Jolos, and F. Döna, Nucl. Phys. **A224**, 93 (1974).

<sup>27</sup> V. Paar, S. Brant, L. F. Canto, G. Leander, and M. Vouk, Nucl. Phys. **A378**, 41 (1982).

<sup>28</sup> V. Paar, in *Interacting Bosons in Nuclear Physics*, edited by F. Iachello (Plenum Press, New York, 1979), p. 163.

<sup>29</sup> S. Brant, V. Paar, and D. Vretenar, Computer code IBFFM/OTQM IKP, Jülich, 1985, unpublished.

<sup>30</sup> A. Passoja, R. Jolin, J. Kantele, J. Kumpulainen, M. Luontama, and W. Trzaska, Nucl. Phys. **A438**, 413 (1985); M. L. Halbert, Nucl. Data Sheets **28**, 179 (1979).

<sup>31</sup> N. J. Ward and J. K. Tuli, Nucl. Data Sheets **47**, 135 (1986); K. Nilson, L. Spanier, B. Erlandsson, K. Vierinen, K. Eskola, and S. Savolainen, Nucl. Phys. **A475**, 207 (1987).

- <sup>32</sup> J. N. Mo and S. Sen, Nucl. Data Sheets **39**, 741 (1983).
- <sup>33</sup> W. W. Daehnick, S. Shastri, M. J. Spisak, and D. Gur, Phys. Rev. C **15**, 1264 (1977).
- <sup>34</sup> M. R. Bhat, Nucl. Data Sheets **55**, 1 (1988).
- <sup>35</sup> M. R. Bhat, Nucl. Data Sheets **58**, 1 (1989).
- <sup>36</sup> M. R. Bhat, Nucl. Data Sheets **68**, 117 (1993).
- <sup>37</sup> M. R. Bhat, Nucl. Data Sheets **68**, 579 (1993).
- <sup>38</sup> M. A. J. Marisotti, M. Behar, A. Filevich, G. García Bermúdez, A. Hernández, and C. Kohan, Nucl. Phys. **A260**, 109 (1976).
- <sup>39</sup> M. M. King, Nucl. Data Sheets **56**, 1 (1989).
- <sup>40</sup> M. M. King and W.-T. Chou, Nucl. Data Sheets **69**, 857 (1993).
- <sup>41</sup> G. García Bermúdez, M. Behar, A. Filevich, and M. A. J. Mariscotti, Phys. Rev. C **14**, 1776 (1976).
- <sup>42</sup> R. Fournier, T. H. Hsu, J. Kroon, B. Hird, and G. C. Ball, Nucl. Phys. **A188**, 632 (1972).
- <sup>43</sup> B. Rosner, S. Mordechai, and D. J. Pullen, Nucl. Phys. **A206**, 76 (1973).
- <sup>44</sup> A. Hübner, Z. Phys. **183**, 25 (1965).
- <sup>45</sup> H. Bertsch, H. Kluge, U. Leithäuser, E. Recknagel, and B. Spellmeyer, Nucl. Phys. **A249**, 93 (1975).
- <sup>46</sup> W. Hogervorst, H. A. Helms, G. J. Zaal, J. Bouma, and J. Blok, Z. Phys. A **294**, 1 (1980).
- <sup>47</sup> J. Döring, S. L. Tabor, J. W. Holcomb, T. D. Johnson, M. A. Riley, and P. C. Womble, Phys. Rev. C **49**, 2419 (1994).
- <sup>48</sup> V. Paar, Nucl. Phys. **A211**, 29 (1973).
- <sup>49</sup> P. Raghavan, At. Data Nucl. Data Tables **42**, 189 (1989).
- <sup>50</sup> T. Bădică, V. Cojocaru, D. Pantelici, I. Popescu, and N. Scînteii, Nucl. Phys. **A535**, 425 (1991).
- <sup>51</sup> B. O. Ten Brink, J. Akkermans, P. Van Nes, and H. Verheul, Nucl. Phys. **A330**, 409 (1979).
- <sup>52</sup> K. Kimura, N. Takagi, and M. Tanaka, Nucl. Phys. **A272**, 381 (1976).
- <sup>53</sup> J. Vervier, P. Van Isacker, J. Jolie, V. K. B. Kota, and R. Bijker, Phys. Rev. C **32**, 1406 (1985).
- <sup>54</sup> D. Čule and V. Paar, Fizika **20**, 99 (1988).
- <sup>55</sup> P. Van Isacker and J. Jolie, Nucl. Phys. **A503**, 429 (1989).
- <sup>56</sup> B. Singh and D. A. Viggars, Nucl. Data Sheets **51**, 225 (1987).
- <sup>57</sup> B. Singh, Nucl. Data Sheets **60**, 735 (1990).
- <sup>58</sup> L. Pfeiffer, T. Kovács, G. K. Celler, J. M. Gibson, and M. E. Lines, Phys. Rev. B **27**, 4018 (1983).
- <sup>59</sup> A. Arima, J. Phys. Soc. Jpn. Suppl. **34**, 205 (1973).
- <sup>60</sup> I. S. Towner, F. C. Khanna, and O. Häusser, Nucl. Phys. **A277**, 285 (1977).
- <sup>61</sup> U. Mayerhofer, T. von Egidy, J. Jolie, H. G. Börner, G. Colvin, S. Judge, B. Krusche, S. J. Robinson, K. Schreckenbach, S. Brant, and V. Paar, Z. Phys. A **341**, 1 (1991).

This article was published in English in the original Russian journal. It is reproduced here with stylistic changes by the Translation Editor.